WILLIAM LETTIS & ASSOCIATES, INC.

Final Technical Report

Surface deformation produced by the 1999 Chi-Chi (Taiwan) earthquake and interactions with built structures

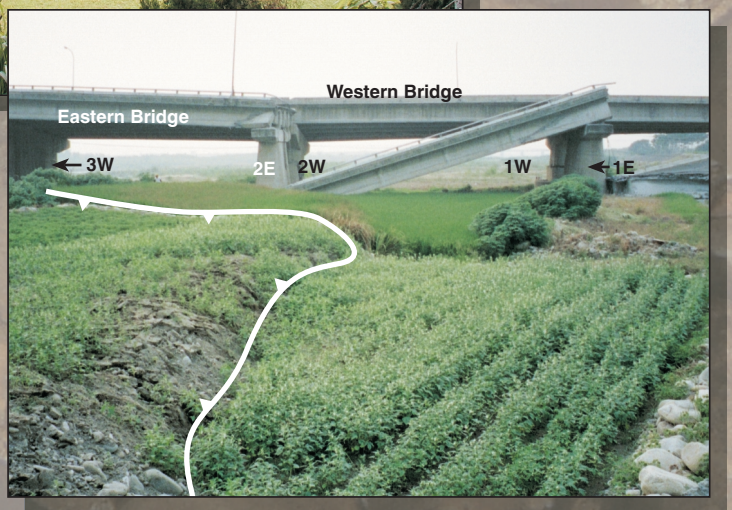

Submitted to:

U. S. Geological Survey
National Earthquake Hazards
Reduction Program
Award Number 01-HQ-GR-0122

Submitted by:

William Lettis & Associates, Inc.
1777 Botelho Dr., Suite 262,
Walnut Creek, CA 94596

December 2003

WLA

FINAL TECHNICAL REPORT

SURFACE DEFORMATION PRODUCED BY THE 1999 CHI-CHI (TAIWAN) EARTHQUAKE AND INTERACTIONS WITH BUILT STRUCTURES

Recipient:

William Lettis & Associates, Inc.
1777 Botelho Dr., Suite 262, Walnut Creek, CA 94596
Phone: (925) 256-6070; Fax: (925) 256-6076

Principal Investigators:

Keith I. Kelson[1], Rich D. Koehler[1], Keng-Hao Kang[1], Jonathan D. Bray[2], and Lloyd S. Cluff[3]

Program Element II
Quaternary Fault Behavior, Rupture Characteristics, Building Response

U. S. Geological Survey
National Earthquake Hazards Reduction Program
Award Number 01-HQ-GR-0122

December 2003

Research supported by the U.S. Geological Survey (USGS), Department of the Interior, under USGS award number (William Lettis & Associates, Inc., 01-HQ-GR-0122). The views and conclusions contained in this document are those of the authors and should not be interpreted as necessarily representing the official policies, either expressed or implied, of the U.S. Government.

[1] William Lettis & Associates, Inc., 1777 Botelho Dr., Suite 262, Walnut Creek, CA 94596 kelson@lettis.com
[2] Department of Civil and Environmental Engineering, Univ. of California, Berkeley, CA 94720 bray@ce.berkeley.edu
[3] Geosciences Department, Pacific Gas & Electric Company, San Francisco, CA 94105 LSC2@pge.com

Award No. 01-HQ-GR-0122

SURFACE DEFORMATION PRODUCED BY THE 1999 CHI-CHI (TAIWAN) EARTHQUAKE AND INTERACTIONS WITH BUILT STRUCTURES

Keith I. Kelson, Rich D. Koehler, and Keng-Hao Kang
William Lettis & Associates, Inc., 1777 Botelho Dr., Suite 262, Walnut Creek, CA 94596
Phone: (925) 256-6070; Fax (925) 256-6076; kelson@lettis.com

Jonathan D. Bray
Department of Civil and Environmental Engineering, Univ. of California, Berkeley, CA 94720
(510) 642-9843; (510) 642-7476 fax; bray@ce.berkeley.edu

Lloyd S. Cluff
Geosciences Department, Pacific Gas & Electric Company, San Francisco, CA 94105
(415) 973-2791; (415) 973-5778 fax; LSC2@pge.com

ABSTRACT

The 1999 **M**7.6 Chi-Chi earthquake produced ground rupture along nearly 90 km of the Chelungpu fault. The rupture traversed densely populated areas and provides an unprecedented opportunity to understand how surface fault rupture may affect buildings. We document the pattern of ground deformation along the fault at several sites that experienced surface fault rupture. While building damage at some sites was severe, other sites along the fault, surprisingly, experienced relatively little building damage. These results help explain why some locales and some buildings are more (or less) susceptible to severe damage from surface fault rupture. At KuangFu Middle School, a single well-defined fault rupture splays into three distinct west-stepping *en echelon* strands that go around or through several severely damaged buildings. The locations of and displacements on the strands vary relative to the locations, types, and orientations of the buildings. Borehole data suggest that the pre-1999 fault location differs slightly from the 1999 surface rupture, which also suggests that the building locations and orientations may have influenced the pattern of shallow rupture. In WuFeng, the thrust front wrapped around the undamaged Suncue Factory building, and had greater hanging-wall folding where it impinged upon the factory. Lesser buildings on the hanging wall collapsed as a result of the amplified folding. This pattern of deformation appears to be related to the massive character of the building, but also to the orientation of the building roughly parallel to the tectonic transport direction and the unconsolidated nature of near-surface materials. Similarly, near Tsaotun, a single fault scarp projects directly toward a 9-m-wide, 27-m-high concrete water tower. At the tower, the scarp wraps around the eastern side of the tower, where anticlinal deformation of the hanging wall is greater. North of the tower, deformation splays into a zone of distributed folding and faulting with much less hanging-wall damage. The presence of the tower

apparently affected the distribution and style of surface deformation. However, the tower was not damaged during the earthquake, and remains vertical despite the deflection of the fault scarp around its base. In contrast, circular pier foundations of the Highway 3 Bridge over the Wu Hsi were severely damaged by the surface rupture where it passes through the bridge structure. The damage to the piers, which have 16-m-deep caisson foundations, was much greater than that to the water tower, which has a foundation only 2.5 m deep. The difference in structural damage between these two sites illustrates the importance of siting structures on the footwall rather than across the fault trace. In conclusion, these sites show that the location, orientation, and type of buildings may influence patterns of shallow deformation (and damage to adjacent buildings).

(Non-technical Summary)

This research provides geologic data to help address how the ground along a fault rupture deforms and affects nearby buildings. We document the pattern of ground deformation at four sites along the Chelungpu fault that experienced severe to moderate faulting as a result of the **M**7.6 Chi-Chi earthquake on September 21, 1999. We compare the characteristics of this deformation with the style and amount of damage that occurred to several buildings at these sites. The results show that some positions along the fault rupture are extremely hazardous but, surprisingly, other positions may not result in severe building damage. This work helps define why some locales and some buildings are more (or less) susceptible to severe damage from surface fault rupture.

TABLE OF CONTENTS

LIST OF FIGURES

1.0 INTRODUCTION

The primary goal of this investigation is to evaluate the effects of ground deformation from the 1999 Chi-Chi earthquake on several buildings and other structures along the fault rupture. Because the earthquake produced surface rupture through densely populated areas, it provides an unprecedented opportunity to advance the understanding of the effects of surface fault rupture on engineered systems. Surface fault rupture represents a significant hazard to a number of U.S. cities, including the greater Los Angeles area, the San Francisco Bay area, Seattle, Salt Lake City, Albuquerque, El Paso, and others. In particular, large reverse faults similar to the Chelungpu fault are present in the greater Los Angeles and San Francisco Bay urban areas. Understanding the style of ground deformation and effects on engineered structures from the Chi-Chi earthquake is critical for evaluating the hazard from reverse faults in urban areas of the United States. The Chi-Chi earthquake produced surface rupture through densely populated areas, and resulted in severe damage to numerous bridges, buildings, utilities and a large dam. The observations of damage resulting from these occurrences have a great potential to redefine U.S. practice in terms of zoning policies and surface fault-rupture mitigation measures. For example, because the Chelungpu fault resembles, in part, many faults in metropolitan areas of southern California, patterns of deformation documented from the 1999 Chi-Chi earthquake may be relevant for assessing Alquist-Priolo Special Studies Zones and for interpreting expected patterns of deformation if these faults were to produce surface rupture. This research will help reduce future earthquake losses by contributing to the understanding of the relationships between geologic deformation and built structures.

Our objectives in this research are to document the style of surface deformation from the Chi-Chi earthquake at a few specific locations, and to identify relationships or patterns between the style of geologic deformation, geotechnical conditions, and damage to built structures at these locations. This effort intends to provide geologic and geotechnical information useful for developing appropriate zoning schemes and improving earthquake-resistant building designs for areas containing active reverse faults with surface-rupture potential. This research builds on our initial post-earthquake studies along the northern part of the 1999 surface rupture (Kelson et al., 2001a, 2001b), and involves an integrated approach toward evaluating the effects of fault-related geologic deformation on buildings and other engineered facilities by combining investigative approaches from the fields of geotechnical engineering and engineering geology. We conducted geologic and geotechnical activities at several sites along the rupture that represent typical styles of deformation along the surface rupture. At each site, our activities included documentation of geologic conditions via detailed surveying and mapping and qualitative assessment of building damage. The results from this effort are applicable to engineering analyses designed to improve hazard mitigation and develop better building designs. We anticipate that the results of this study will provide guidance for developing or revising fault-rupture zonation policies for metropolitan areas in the United States that are exposed to surface rupture along active reverse faults.

2.0 GEOLOGIC AND GEOTECHNICAL BACKGROUND

2.1 Geologic Framework

The 1999 Chi-Chi earthquake (M_W 7.6) occurred along the Chelungpu thrust fault in central Taiwan, resulting in about 100 km of surface rupture (Figure 1). Seismological analyses suggest the earthquake occurred on a shallow dipping (≈ 30˚) fault that strikes about N26˚E, with a hypocentral depth of about 7 km (Ma et al., 1999). Analysis of mainshock seismograph records suggests that the rupture initiated down-dip from the town of Nantou and propagated bilaterally, extending about 35 km southward through Chushan and about 65 km northward to the Tachia River valley. The maximum subsurface fault dislocation of about 10 meters appears to have occurred about 30 to 45 km north of the hypocenter, down-dip from the town of Wufeng (Figure 1). These rupture characteristics appear to have influenced the pattern of surface deformation, and thus the distribution of building damage and losses related to the earthquake.

The 1999 Chi-Chi earthquake and subsequent aftershocks destroyed approximately 8,500 buildings and significantly damaged another 6,200. Damage was heaviest in the central Taiwan counties of Taichung, Nantou, and Yuanlin, which are traversed by the Chelungpu fault. Compared to other historic earthquakes throughout the world, there was an unusually large percentage of building damage related specifically to surface fault rupture during the Chi-Chi earthquake. Damage related directly to surface rupture typically is responsible for less than about 5% of losses; whereas losses associated directly from surface ruptures during the Chi-Chi earthquake is estimated to be as high as 35% to 50%. The general pattern of damage closely follows the surface rupture throughout the length of the fault. Importantly, the distribution of damage to buildings and other facilities appears to be strongly influenced by the distribution of surface faulting, with greater amounts of damage along the primary surface-rupture scarp and within the hanging wall east of the scarp (Kelson et al., 2001a, 2001b).

The pattern of surface deformation from the 1999 earthquake varies substantially along the length of the Chelungpu fault (Azuma et al., 1999; Chen et al., 1999; Chen and Chen, 1999; Lee et al., 1999; Kelson et al., 2000a, b). Along the southern part of the rupture, the reverse fault scarp is generally 1 to 3 m high, and is associated with local hanging-wall folding. Along the central part of the rupture, fault scarps are higher (generally about 2 to 4 m high) and are associated with a broader zone of deformation in the hanging wall. In contrast, the northern part of the rupture is associated with scarps as much as 5.5 m high as well as complex folding and secondary faulting on the hanging wall. Importantly, the variability in the style and amounts of surface deformation produced by this earthquake demonstrate that ground deformation associated with large reverse earthquakes can be difficult to predict at any specific location, especially at sites on the complexly deformed hanging wall adjacent to primary fault traces (Kelson et al., 2001b).

During our earlier efforts, we focused on documenting characteristics of the surface faulting along the central and northern parts of the Chelungpu fault, from Wufeng to Cholan (Figure 1; Kelson et al., 2001b). These investigations show that the location and style of geologic deformation appears to have affected the location and style of damage to buildings and other

facilities. In general, there was relatively little building damage (related to surface-rupture processes) on the footwall, severe damage on the main fault scarp itself, and distributed moderate damage on the hanging wall. Nearly all of the damage to buildings located on the footwall appears to be related to "bulldozing" of the hanging-wall material onto the footwall.

The most severe geologic deformation (and thus building damage) associated with surface rupture along the northern part of the Chelungpu fault occurred along the primary reverse-fault scarp. Substantial damage nearly always occurred to buildings or other structures spanning the fault rupture, as a result of differential vertical movement, severe tilting and/or westward translation (Kelson et al., 2001a). As might be expected, buildings with thin concrete-slab foundations generally sustained severe damage where located on the fault scarp (i.e., Figure 2a). Although several buildings with massive, reinforced foundations were damaged along the fault, there are examples of such structures undergoing severe tilting without collapse (Figure 2b), or vertical uplift without severe internal deformation (Figure 2c). Rarely, buildings spanning the fault rupture were able to withstand surface displacement without collapse (Figure 3).

Although geologic deformation and consequent building damage appear to be greatest along the primary fault scarp, there also was substantial faulting, folding, and tilting on the hanging wall. Most zones of deformation on the hanging wall are less than a few hundred meters wide, but some localities experienced deformation as much as 1.5 km east of the west-facing fault scarp. In general, the 1999 earthquake produced three distinct types of ground deformation on the hanging wall: (1) secondary fault rupture and associated minor anticlinal folding, (2) regional tilting across a wide zone, and (3) axial surface deformation where the ground surface (and buildings) passed through the hinge of a growing anticline during ground movement. These types of deformation produced various degrees of damage to buildings, facilities, and lifelines, from minor cracking to tilting to severe damage or collapse. On the basis of these previous studies (Kelson et al., 2000a, 2000b, 2001a, 2001b) and additional detailed documentation developed during this investigation, we believe that the style and locations of deformation, both along the fault scarp and on the hanging wall, strongly influenced the pattern of damage to buildings and other structures.

2.2 Geotechnical Framework

Sherard et al. (1974) showed that integration of engineering geology and geotechnical engineering principles is critical to the successful development of appropriate fault-rupture mitigation strategies. Since publication of this landmark paper, several investigators have developed strategies and analytical procedures for evaluating the effects of surface fault rupture on engineered structures (e.g., Lade and Cole, 1984; Youd, 1989; Bray et al., 1993a, 1993b, 1994b; Lazarte et al. 1994, Lazarte and Bray 1996, Murbach et al. 1999). These efforts show that the characteristics of surface faulting depend greatly on the thickness and nature of the soil materials overlying the fault, as well as the fault type, dip of the fault, and amount of fault displacement. For instance, for a particular level of displacement across a distinct bedrock fault, the height that the rupture will propagate into the overlying soil is primarily a function of the ductility of the soil. Field and laboratory studies have shown that ductile earth materials can accommodate significant fault movement by warping without developing distinct shear surfaces (e.g., Bray et al. 1993a, 1994a). In addition, fault type, dip, and amount of movement also play important roles, with reverse faults tending to gradually decrease in dip near the ground surface,

producing secondary ground deformation in a broad area on the hanging wall. During the 1999 Chi-Chi earthquake, reverse displacement produced a broad range of styles of ground deformation, including primary fault rupture, tilting and warping, and a variety of secondary fault ruptures on the hanging wall (Kelson et al., 2001b). In order to understand the complexity of the ground rupture with respect to engineered structures, an integrated approach that combines geologic and geotechnical information is necessary and appropriate.

Analytical techniques developed as part of continuing engineering research efforts have been applied to mitigation of rupture hazards and seismically resistant building designs. Field data available from the 1999 Chi-Chi earthquake provide an opportunity to test the reasonableness of these analytical techniques. For example, the interaction between structural foundations and surface faulting was examined in a limited way for the surface rupture produced by the 1992 Landers earthquake. However, the 1992 rupture occurred through a sparsely populated region, and only a few examples of rupture through engineered facilities were available for study (Lazarte et al., 1994). In contrast, much of the 1999 Chi-Chi rupture traversed highly urbanized areas, providing a unique set of conditions that allows for an evaluation of the effects of surface rupture on engineered facilities. Our documentation of ground deformation along the Chelungpu fault, and its resulting effect on different types of structural systems, enhances the understanding of how reverse faults affect the built environment.

3.0 GEOLOGIC SITE CHARACTERIZATIONS

This research was designed to characterize the geologic conditions at selected sites along the Chelungpu fault, and compare these characteristics with qualitative assessments of building damage. In general, documentation of geologic conditions involved detailed topographic surveying and geologic mapping of deformation-related features at selected representative sites. Our investigation focused on collecting geologic information at four sites along the west-vergent Chelungpu thrust fault rupture: (1) the KuangFu Middle School in WuFeng, (2) the Experimental Vineyard site in WuFeng, (3) the Municipal Water Tower near Tsaotun, and (4) the Highway 3 Bridge over the Wu Hsi (River). All four of the sites include structures that are either traversed by the surface rupture or are directly adjacent to the fault scarp. The first two sites include buildings affected by the surface rupture, and the second two sites include either piers or a circular tower foundation. The results from our investigations at these sites are described below.

3.1 KuangFu Middle School, WuFeng

KuangFu Middle School is along the central part of the Chelungpu fault about 4 km southeast of central WuFeng (Figure 1). The school is on a 4-m-high late Holocene fluvial terrace flanking the northern margin of the Gan Hsi (River) (Figure 4). The coarse gravel terrace deposits rest upon shale of the Pliocene Chinshui Formation, are about 5 m thick on the hanging wall and more than 12 m thick on the footwall. The Chelungpu fault scarp strikes northwesterly through the school campus, and was unmodified at the time of our surveying in September 2001. Because the school rests on a very young stream terrace, the site contains geomorphic evidence of only the 1999 rupture. Within the vicinity of the school, the 1999 Chelungpu fault rupture is predominantly a single fault scarp across the Gan Hsi valley, except for the presence of three localized strands within the Kuangfu Middle School site (Figure 4).

The deformed track at the KuangFu Middle School has received abundant attention, in part because the surface deformation is strikingly clear (i.e., http://geot.civil.metro-u.ac.jp/archives/eq/99taiwan/) (Figure 5). As part of our early post-earthquake efforts in characterizing the fault-related surface deformation (Kelson et al., 2001a), detailed topographic surveying of the N45˚W-trending fault scarp where it crosses the track and field showed a net vertical tectonic displacement (NVTD) of 2.8 $\pm$ 0.5 m. We also noted that this single scarp splits into three strands in the area north of the track, where the fault zone crosses the school campus. The total NVTD of the fault zone through the school and along a road bordering the northern margin of the school is comparable to that at the track (Kelson et al., 2001a). Additional reconnaissance of the school campus showed that buildings and other structures located on the hanging wall but more than about 40 m from the fault scarp experienced minor or no damage (Kelson et al., 2001b). Because the severity of damage to school buildings on the footwall is atypical, Kelson et al. (2001b) speculated that westward thrusting of buildings located astride the fault scarp impacted the adjacent buildings on the footwall, resulting in damage or collapse of the footwall buildings. In addition, we noted that specific buildings were spatially associated with fault bifurcations, and speculated that the "Eastern Classroom Building" (see Figure 6) might have influenced the pattern of surface fault rupture and contributed to the occurrence of multiple strands in and north of the campus.

Our subsequent effort (reported herein) was designed to test the hypothesis that the location, orientation, and/or structural characteristics of the Eastern Classroom Building might have influenced the pattern of surface fault rupture through the school campus. Our approach involved two lines of investigation. First, we delineated the exact pattern and style of surface deformation with respect to the building location, to test the possibility of a spatial association between the rupture strands and the school buildings. Second, we collected borehole data to evaluate the subsurface location of the pre-1999 fault strand, and thus to assess whether the location of the 1999 surface rupture is spatially coincident with the pre-1999 fault trace. We reasoned that if the 1999 rupture location differs substantially from the pre-1999 fault trace, and if there is a spatial association between the school buildings and the 1999 surface rupture, then the buildings may have influenced the location and pattern of surface deformation. The results of this investigation are described below.

3.1.1 Detailed Delineation of Surface Deformation

We constructed a detailed topographic map of the fault strands and buildings on the school campus in September 2001, using a Topcon GTS-303 electronic total station (Figure 6). This survey extends from the single, N45˚W-trending fault scarp at the northwestern corner of the track, along the fault scarps through campus, and to the asphalt roadway directly north of campus. Near the southeastern corner of campus, the fault scarp has a NVTD of about 3 m (Figure 7). Upon traversing a highly deformed, north-trending concrete walkway along the eastern margin of the campus, this large scarp abruptly splits into two smaller fault scarps (Figure 6). The eastern fault scarp extends along a N10˚W direction until it encounters the eastern wall of the two-story Eastern Classroom Building, and then it extends along the building wall with a N15˚E orientation (Figure 6). Topographic profiles across this scarp show that it decreases slightly in height progressively from about 0.9 m NVTD on the south to about 0.6 m NVTD on the north (Figures 7b and 8). Our previous, low-resolution topographic profile along the road north of campus estimated a NVTD across this scarp of about 0.7 m (Kelson et al., 2001a). Near the center of the Eastern Classroom Building, the rupture clearly impinged upon the eastern wall, causing structural damage to several of the building columns and collapse of a concrete patio roof. This scarp continues northward across the road, where it resulted in severe damage to one-story residential buildings (Kelson et al., 2001b) (Figure 9).

The southern end of the Eastern Classroom Building is severely damaged as a result of deformation associated with the western and central strand of the fault (Figures 5 and 10). The southernmost part of the building essentially overlies the western fault scarp, as reflected by the tilts of the building floor, which range up to 8.5˚ to the southwest (Figure 6). The fault tip wraps around the southern end of the building, and extends westward to the northeastern corner of the adjacent “Southern Classroom Building” (e.g., “Building C” of Kelson et al., 2001b). The entire Eastern Classroom Building is tilted southwestward, with the degree of tilting decreasing progressively from 8.5˚SW at its southern end, to about 1.5˚SW in a central classroom, to about 0.2˚W in a northern classroom. This pattern of tilting may be related to deformation along the eastern fault strand (which borders the eastern margin of the building) and/or the central fault strand (which borders the western margin of the building) (Figure 6). Notably, the two-story Eastern Classroom Building contains a limited subsurface basement, located only at its southernmost end.

The central fault strand extends along the western side of the Eastern Classroom Building, branches northwestward into the campus quadrangle with a strike of about N25˚W, and extends to the asphalt roadway north of campus. Topographic profiles across the central fault strand show a NVTD of about 0.6 to 0.7 m (Figures 7b and 8). A northward decrease in the NVTD along this strand is indicated by our previous measurement of only 0.3 m of NVTD along the asphalt roadway (Kelson et al., 2001a). North of the roadway, we were unable to map the central fault strand because of disturbances related to demolition of a one-story residential building that was damaged during the earthquake (Kelson et al., 2001b). We speculate that this strand may merge with the western fault strand to the north of our study area, or that the strain is transferred to this strand through distributed deformation of the hanging wall.

As noted above, the southernmost end of the Eastern Classroom Building essentially overlies the western and central fault scarp. The western scarp continues northwestward through the school campus, and has a sinuous trace with an average strike of about N50˚W (Figure 6). Upon exiting the Eastern Classroom Building, the tip of the western strand continues westward to the northeastern corner of the Southern Classroom Building, and then bends abruptly to the northwest. Overall, the trace of the fault tip in the southeastern part of the school campus appears to have encountered the Eastern Classroom Building, wrapped around its southern end, encountered the Southern Classroom Building, and then regained a northwesterly orientation (Figure 6). Directly north of the Southern Classroom Building, the fault scarp has a moderate amount of NVTD (0.8 m, Figure 7b), which represents about one-third of the total NVTD across the fault zone. Along Profile BB', the total uplift is distributed equally among the western, central and eastern fault strands. Where the western fault strand traverses the landscaped quadrangle in the central part of campus, it gradually increases in height to the north, having about 1.0 m of NVTD (Figure 8a). There is no evidence of ground deformation west of this fault strand, although the hanging wall of this strand exhibits some gentle deformation. This is best shown by a series of four irregular-shaped concrete planter boxes that are aligned across the fault scarp. These boxes show different amounts of tilt according to location with respect to the fault scarp. Our detailed surveying shows that the two planter boxes west of the fault are horizontal and undeformed, whereas the planter box east of the fault is gently warped and has a tilt of about 1.1˚ west. The planter box that lies astride the fault scarp (Figure 6) is broken, shortened, and severely deformed. As with many linear features crossed obliquely by the fault, the locally southwesterly vergence of the thrust fault generated an apparent right-lateral displacement of these planters (Figure 6). These planter boxes are highly representative of the styles of deformation commonly observed along the 1999 rupture of the Chelungpu fault, as summarized by Kelson et al. (2001b): little or no deformation on the footwall, severe damage along primary and secondary fault scarps, and gentle to moderate tilting or folding on the hanging wall within tens of meters of fault scarps.

Perhaps one of the most graphic examples of building damage related to surface-fault rupture from the 1999 earthquake is the three-story classroom building in the northern part of campus (Figure 11a). The western fault strand traverses this building, which experienced total collapse on the hanging wall, and severe deformation and shortening at the fault crossing (Figure 11b). On the footwall, the building experienced severe structural damage and partial collapse probably related to the shortening and westward thrusting of the building's structural elements. The orientation of the western fault strand on the southern side of the building is about N50˚W, but

its orientation on the northern side of the building is approximately north, which is similar to the change in fault strike where the fault strand encountered the Southern Classroom Building (Figure 6). Topographic profiling across the fault scarp north of the Northern Classroom Building shows that the NVTD is about 1.4 m near the building (Figure 8b), and about 2.2 m along the road north of the campus (Kelson et al., 2001a). Therefore, the NVTD along the western strand increases gradually across the campus from south to north.

Overall, the total NVTD across the entire fault zone at KuangFu Middle School is consistent from north to south, ranging from about 2.4 to 2.6 m. This is consistent with the total NVTD of 2.8 $\pm$ 0.5 m measured by our earlier effort at the adjacent track and field (Kelson et al., 2001b). However, the distribution of uplift changes among the various fault strands at the site, with the eastern and central fault scarps gradually decreasing in height from south to north, and the western fault scarp increasing in height from south to north. Thus, it appears that in a general sense, uplift along the fault is transferred from the eastern and central strands to the western strand progressively from south to north. Although the exact mechanism of this transfer is not known, it likely occurs through distributed strain (e.g., folding, warping, uplift) in areas between the major fault strands. In addition, our field reconnaissance north of the campus shows that the eastern and central fault strands gradually die out in a northerly direction, and that the western fault strand continues northward as a single, dominant surface rupture. Thus, the presence of three fault strands at the Kuangfu Middle School campus is a local characteristic that is anomalous along a predominantly single fault scarp in the vicinity of WuFeng.

3.1.2 Shallow Borehole Data

As noted above, we collected borehole data to evaluate the subsurface location of the pre-1999 fault strand, and thus to assess whether the location of the 1999 surface rupture is spatially coincident with the pre-1999 fault trace. We reasoned that if the 1999 rupture location differs substantially from the pre-1999 fault strand, and if there is a spatial association between the school buildings and the 1999 surface rupture, then the buildings may have influenced the location and pattern of surface deformation. To this end, we collected data from six shallow boreholes previously completed on the school campus and the track and field (J. Sun, Pacific Gas & Electric Company, written communication, 2001), and we completed two shallow boreholes on the school campus in September 2001 (Figure 6).

The six previous boreholes were completed on both sides of the primary (western) fault strand, and show a distinct difference in the depth to bedrock across the fault strand. Boreholes B-2 and B-4 were drilled on the eastern side of the western fault strand, and encountered coarse fluvial gravel from the ground surface to depths of 5.3 m and 5.2 m, respectively (Figure 6). Below the gravel is the soft, grey shale of the Chinshui Formation, which is easily identified on the basis of color, texture, and decreased drilling pressure. In contrast, previous boreholes B-1, B-3, B-5, and B-6 all encountered only the coarse fluvial gravel to the depth of investigation, which ranged from 6 to 7m (Figure 6).

Similarly, we drilled one borehole on either side of the western fault strand in the center of the school campus (boreholes WLA-4 and WLA-5; Figure 6). These boreholes were sampled continuously using a split-spoon coring device. Borehole WLA-4 encountered coarse fluvial gravel to the depth of investigation (7 m), and borehole WLA-5 encountered this same gravel to

the depth of 12 m. The gravel contains rounded clasts consisting of coarse-grained sandstone, greywacke, and limestone lithologies. Neither borehole encountered the distinct grey Chinshui Shale.

Based on our field observations of fluvial gravel deposits and associated strath terrace surfaces cut onto the Chinshui Shale at many locations along the mountain front of the Western Foothills, the bedrock strath surfaces consistently have very little relief (less than about 0.5 m). This may be related to the high erodibility of the shale and the high stream power of the west-flowing rivers (as indicated by gravels dominated by boulder and cobble clasts). From this, we interpret that east of the Chelungpu fault trace beneath Kuangfu Middle School, the bedrock strath surface is about 5.2 or 5.3 m deep. The absence of a pre-1999 fault scarp across the school campus suggests that the Gan River deposited the uppermost, 5-m-thick gravel following the penultimate surface rupture on the fault, and that thicker sections of fluvial gravel reflect burial of the downthrown side of the fault. We use this information to infer the pre-1999 location of the Chelungpu fault beneath the Kuangfu Middle School. We interpret that the 5-m-thick section of gravel encountered in boreholes B-2 and B-4 is the youngest, pre-1999 strath deposit, and that these two boreholes are located east of the pre-1999 fault trace. In contrast, the thick section of gravel encountered in boreholes B-1, B-3, B-5, and B-6, and in our boreholes WLA-4 and WLA-5 all represent deposits that are west of the pre-1999 fault trace. Based on this information, the pre-1999 fault trace is located between boreholes B-4 and WLA-4 (Figure 6). Because borehole WLA-4 is located on the hanging wall of the western fault strand (Figure 6), we interpret that this strand represents a "new" surface rupture, meaning that this strand was not present prior to the 1999 surface rupture. We speculate that if the 1999 earthquake had ruptured the surface along the pre-existing fault trace at the school, it would have extended directly through the Eastern Classroom Building, rather than around its southern end and then through the central part of the campus.

3.1.3 Interpretation of Patterns of Ground Deformation and Building Damage

On the basis of the survey and borehole data, we interpret that the patterns of ground deformation and building damage at the Kuangfu Middle School are intimately related. In particular, it seems that the location and orientation of the buildings may have influenced the pattern of ground rupture produced by the 1999 earthquake. First, the Chelungpu fault in the site vicinity is primarily a single fault strand, with the exception of the three scarps that traverse the school campus, suggesting that the three rupture scarps through the campus are unique. Second, two of the scarps are secondary strands that die out to the north, such that the total uplift is transferred back to the single western fault strand present north of the campus. Third, the pre-1999 trace of the fault differs from the 1999 rupture locally where it encounters the school buildings, suggesting that the pattern of the 1999 rupture is different from previous rupture patterns. And lastly, the location and character of the scarps through the campus appear to be influenced by the building locations and orientations. This last point is supported by the northerly strike of the eastern strand where it parallels the Eastern Classroom Building and the Principal's Quarters (Figures 4 and 6), and by the map pattern of the fault tip as it wraps around the southern end of the Eastern Classroom Building (Figure 6). Additional support includes the abrupt changes in strike of the western strand from westerly to northwesterly at the corner of the Southern Classroom Building, and from northwesterly to northerly where the fault encounters the Northern Classroom Building (Figure 6).

The orientations and structural characteristics of the classroom buildings may have significantly affected how the rupture and the buildings interacted. For example, the angle between the fault and the Eastern Classroom Building in the southeastern corner of the campus is oblique (about 70˚), such that a minor part of the strain could be accommodated by deformation along the long axis of the building and some could be taken up across the southern end of the building (Figure 6). Damage to this building was severe because it spanned the fault scarp at its southern end, and because of impingement of material bulldozed against the building by the eastern fault strand. Tilting of this building and of the Principal's Quarters likely was related to distributed deformation on the hanging wall of the central fault strand. Notably, the southern end of the Eastern Classroom Building contains a basement, which may have acted as an anchor for the entire structure as it experienced southwestward thrusting. We are unclear as to whether the presence of the basement in this building may have made the damage greater or lesser than if it had no basement.

Nevertheless, we believe that the splaying of the single fault strand into three strands at the southern end of the Eastern Classroom Building is related to the presence of this building. Because the rupture propagated northward toward the school, this was the first building the rupture encountered on the campus. We believe that the mass of the building, and the unconsolidated condition of the underlying fluvial gravel deposit, allowed the thrusted material to deform in the complex pattern mapped on Figure 6. If the building had been founded on bedrock rather than unconsolidated material, the rupture may have been concentrated primarily along the pre-1999 fault trace, rather than secondary splays, and the damage to the building might have been more severe.

3.2 Experimental Vineyard and Suncue Sheet Metal Factory, WuFeng

The Experimental Vineyard site is on the central part of the Chelungpu fault, near the city of WuFeng (Figure 1). The 1999 surface rupture traverses a vineyard developed on a young fluvial terrace underlain by coarse alluvium (Figure 12). Detailed mapping shows that the scarp produced about 2.2 m of net vertical tectonic displacement (NVTD) of the vineyard surface, and about 3.3 m of horizontal shortening (Kelson et al., 2001b). Our previous investigations at the site show that the surface rupture traverses the vineyard but wraps around the southern end of a large factory (Kelson et al., 2001b). We interpreted that the massive concrete foundation of the factory building impeded the northwestward transport of the hanging wall and affected the location and height of the local surface scarp. This resulted in localized folding on the hanging wall, and may have significantly contributed to the severity of damage to single-story residential buildings on the hanging wall. At the Experimental Vineyard site, we collected additional subsurface information to supplement our previous geologic characterization, and we collected data on the characteristics of the massive factory building. The purpose of our investigation was to characterize the near-surface materials that impinged upon the factory building, and to evaluate building conditions that may shed light on the how this particular building was not severely damaged by the surface rupture and, apparently, influenced the location and pattern of the 1999 surface rupture.

3.2.1 Shallow Borehole Data

Additional data collected during our recent efforts includes information from two air-rotary boreholes on the hanging wall of the fault (WLA-1 and WLA-2) and one borehole on the footwall (WLA-3; Figure 12). The boreholes show that the coarse fluvial gravel on the hanging wall is about 5 m thick and overlies shale bedrock of the Chinshui Formation. On the footwall, the coarse gravel is more than 18 m, the total depth of exploration. Because there is no geomorphic evidence of a pre-1999 scarp along the fault at the site, the fluvial system either removed or buried any pre-existing fault scarp prior to the 1999 rupture. The greater depth to bedrock on the footwall suggests that there has been recurrent movement on the fault through the site, which is now occupied by the factory building.

3.2.2 Interpretation of Patterns of Ground Deformation and Building Damage

Our earlier efforts at this site showed that the fault trace wrapped around the factory building, which we interpreted as an indicator that the building was structurally competent and able to withstand the loads imposed by the surface rupture (Kelson et al., 2001b). We speculated that the building may have deflected the fault strand around the southeastern corner of the structure, and thus affected the pattern of surface rupture. Combined with our earlier geomorphic mapping of the Suncue Factory site, we developed additional data on subsurface and building conditions to provide more information on how the building may have affected the rupture pattern. First, data, on column type and spacing, and foundation type, obtained from factory personnel show that the building is moderately strong, but perhaps not as massive or competent as we previously thought. Second, the soil materials above bedrock at the site are primarily cobble-gravel deposits. On the hanging wall, this unconsolidated gravel is about 5 m thick. This is substantially thicker than the total vertical uplift along the fault, which is about 2 to 2.5 m (Kelson et al., 2001b; Figure 13). Therefore, the entire thickness of hanging-wall material that was thrust onto the vineyard surface during the 1999 rupture is composed of unconsolidated granular material. Based on our previous geomorphic mapping, analysis of displaced cultural features, and topographic profiling of the scarp, the 1999 surface rupture at this site produced about 3.3 m of net horizontal shortening (Kelson et al., 2001b). Thus, the gravel material probably was thrust about 3 or 4 m along the vineyard surface. The loads imposed on the factory building, therefore, were transmitted entirely by the gravel material, rather than consolidated bedrock. We suggest that the thickness of the unconsolidated material contributed to the ability of the factory building to withstand the loads imposed by the surface rupture. If the alluvium were less than about 2 m thick at this site, then the uplifted and translated material would have included bedrock, and the response of the building to the imposed load may have been different. In addition, the 5-m-thick alluvium at the surface has a lower strength than bedrock, and thus may have made it easier for the fault strand to steepen (in cross-section) and/or bend (in plan view) to accommodate the building mass. Thus, we interpret that several factors allowed the building to withstand the load imposed by the 1999 surface rupture, including the building's location primarily on the footwall, the moderately competent building foundation, the orientation of the building's long-axis roughly parallel to the thrust vergence direction, and the presence of unconsolidated, granular material in the uplifted and bulldozed hanging wall.

3.3 Municipal Water Tower, Tsaotun

At the Tsaotun Municipal Water Tower site, we conducted detailed topographic surveying and geologic mapping of the fault rupture as it intersects the 9-m-wide, 27-m-high concrete water tower (Figure 14). Directly south of the tower, the fault rupture is expressed as a single, 1.5-m-high west-facing fault scarp that projects northward directly toward the water tower (Figure 15). At the tower, the fault scarp wraps around the eastern side of the tower, where anticlinal deformation of the hanging wall is substantial. A drainage ditch along the eastern margin of the tower is completely closed as a result of shortening. Directly north of the tower, the scarp bifurcates into two scarps within a zone of distributed folding and faulting. In this area, the overall trend of the deformational zone is similar to that south of the tower, and the adjacent drainage ditch is relatively undeformed. Our analysis of the deformation at this site involved constructing a detailed topographic survey of the area and several cross-fault topographic profiles. We also collected as-built plans of the tower from the local water company, which provide information on the tower geometry and its subsurface foundation.

The water tower site is along the Chelungpu fault at the base of a linear, faceted mountain front, and on a high alluvial-fan deposit preserved between two west-trending, incised (20-m-deep) river canyons. Based on exposures elsewhere along the mountain front, the alluvial-fan deposits likely are composed of coarse fluvial gravel, including boulders, cobbles and finer material. The majority of native materials at the surface near the water tower consist of silty sand, although we have no site-specific information on subsurface geologic conditions. The ground surface surrounding the water tower was landscaped, prior to the 1999 earthquake, with sod and irregularly spaced trees (Figure 15). Southwest of the tower and the landscaped area are an asphalt roadway and parking area, which provides access to a series of apartment buildings located about 50 m southwest of the tower. The northeastern margin of the landscaped area is marked by a 3-m-high retaining wall that rises above the site and borders a starfruit-tree orchard on the gently sloping fan surface northeast of the site. Based on our site reconnaissance, this retaining wall extends southeastward across the fan surface for several hundred meters, and likely represents the base of a pre-existing fault scarp developed on the alluvial-fan deposits. We observed no evidence of deformation within the orchard northeast of the site, on the hanging wall side of the fault uphill of the retaining wall. A small concrete drainage ditch (25 cm wide by 50 cm deep) runs along the base of the retaining wall and, prior to the 1999 earthquake, transported runoff to the northeastern corner of the site (Figure 15).

We obtained as-built plans showing the structural characteristics of the water tower from the local municipality. These plans show that the tower consists of a 20.5-m-long, 9-m-diameter concrete cylinder upon which the water tank rests (Figure 14). The water tank is 9 m in diameter, 5 m high, and has an arched roof that is 1.5 m above the high-water level at its central peak (Figure 16). The walls of the tank and supporting cylinder are 25 cm thick, and the total height of the structure above the ground surface is about 27 m. The plans also show the subsurface foundation of the tower to consist of a circular footing that has a total outside diameter of 16 m, and extends to a depth of 2.5 m (Figure 16). Personnel with the municipal water department indicated that there was no water in the tank at the time of the 1999 earthquake. The tower sustained no structural damage as a result of the nearby surface rupture,

and our measurements after the earthquake indicate that the tower remains vertical, and did not sustain any tilting from the earthquake.

Our topographic survey included the vicinity of the water tower, extending from the retaining wall bordering the eastern margin of the site to the southwestern margin of the roadway (Figure 15). The northern limit of the survey area is marked by a 0.5-m-deep concrete drainage ditch and adjacent retaining wall, which rest on the rim of the incised river canyon (Figure 15). The southern limit of the survey area is an arbitrary boundary within an area that was re-graded and disturbed by construction activities following the 1999 earthquake. The Taiwan Central Geological Survey noted that the 1999 earthquake produced a scarp about 0.5 m high through the southernmost part of the site, in the area that has since been re-graded.

Our detailed survey documents the location and character of the 1999 surface rupture through the water tower site (Figure 15). South of the tower, the rupture consists of a single, 1.5-m-high fault scarp that strikes about N35˚W (Figure 17). Topographic profiles across this scarp show that the deformation occurred primarily within a zone about 6 or 7 m wide (Figures 18a and 18b). Using the gentle slope of the landscaped area on the footwall, we estimate a net vertical tectonic displacement (NVTD) of about 0.8 m along both profiles A-A' and B-B'. Assuming a 30˚ northeasterly dip on a primary fault strand that projects upward to the base of the pre-1999 retaining wall, these profiles suggest a net shortening of about 1.3 m at this site. We speculate (as shown on Figure 18) that the dip of the fault decreases in the shallow subsurface, and daylights at the base of the topographic scarp. Based on these profiles, the shallow run-out of the thrust fault onto the pre-1999 ground surface is only a few meters wide. The area on the hanging wall of the fault is folded and deformed, as also illustrated by the presence of tilted betel nut trees along the scarp face (Figure 17). However, the drainage ditch at the base of the retaining wall remained open, in contrast to the ditch where it is adjacent to the tower (see below).

As noted above, the fault scarp projects directly into the base of the water tower, wraps around the eastern side of the tower, and then continues to the northwest (Figure 15). In contrast to the tilted betel nut trees located along the scarp face south of the water tower, the tower itself remains vertical. The soil material between the tower and the retaining wall is severely deformed and forms a sharp-crested hanging-wall anticline (Figure 18c). The drainage ditch along the base of the retaining wall is closed, in contrast to areas north and south of the tower, where it remains open. Based on our topographic profiling, the NVTD at this location along the fault is about 1.1 m, which is slightly more than the NVTD north and south of the tower. Assuming that the net horizontal shortening is the same along the fault scarp, the greater NVTD behind the tower suggests that the very uppermost tip of the fault has a slightly steeper dip (about 36˚) in the local vicinity of the tower (Figure 18c). Because the tower shows no evidence of structural damage or tilting, it appears that the surface rupture had no significant impact on the tower's structural integrity, and instead that the tower itself may have influenced the local style of near-surface deformation.

North of the tower, the fault rupture splits into two strands: a western strand that strikes about N45˚W and an eastern strand that strikes about N25˚W and is parallel to the retaining wall (Figure 15). The total NVTD across the fault zone ranges from 0.6 to 0.9 m along the scarp north of the tower, and the fault tip daylights in the landscaped area along the western fault scarp

(Figure 19). The eastern strand dies out to the north at the boundary of the survey area, where the strain appears to be accommodated by a small anticline and transferred westward to the western fault strand via distributed deformation. Because of the divergent strikes of the two fault strands, the width of deformation increases northward, although it seems likely that the eastern fault strand is a local secondary feature. We speculate that the splitting of the fault into these two strands is related in some way to the northward direction of rupture propagation and the presence of the (ostensibly) immobile water tower, perhaps as a refraction of the rupture as it encountered the tower in the shallow subsurface.

Thus, it appears that the presence of the water tower adjacent to the pre-1999 fault trace may have affected the distribution of deformation at the site. The divergence of the western strand away from the base of the retaining wall (and presumably the pre-1999 location of the fault tip) suggests that the majority of the surface deformation wrapped around the tower and developed farther west than that during previous surface-rupturing events. In addition, the surface rupture did not appear to significantly impact the integrity of the tower. Given that the tower foundation extends only 2.5 m into the shallow subsurface, it seems likely that either: a) the mass of the tower affected the dip of the fault in the very near surface, forcing it to steepen as it reached the ground surface, and/or b) the fault tip is farther east than the base of the retaining wall, and the material deformed behind the tower reflects merely "bulldozed" soil. In the latter case, the soil east of the tower was pushed against the lower 1.5 m of the tower and did not affect the base or foundation of the tower. In this case, as suggested by the complex scarp bordering the northern side of the tower (Figure 15), the bulldozed soil appears to have squeezed around the sides of the tower.

3.4 Highway 3 Bridge Over Wu Hsi, Nantou

The Wu Hsi Bridge is along the central part of the Chelungpu fault, between the cities of Wufeng and Nantou (Figure 1). The bridge is along Highway 3 where it crosses the Wu Hsi (river), which is one of four major rivers that drain the mountain range east of the Chelungpu fault. Mapping of the 1999 surface rupture by the Taiwan Central Geological Survey, National Central University and other workers shows that the Chelungpu fault crosses through the bridge structure near the northern margin of the Wu Hsi channel. As a result of the earthquake, the northern two spans of the northbound lanes collapsed, and the northern two piers supporting the southbound lanes experienced shear failure without collapsing (Kelson et al., 2001b; Figure 20). Our effort at this locality includes detailed topographic surveying and geomorphic mapping of the surface-rupture directly south of, beneath, and north of the Highway 3 bridge, in order to interpret possible interactions between the pattern and style of fault rupture and the bridge structure.

The 625-m-long Highway 3 bridge system over the Wu Hsi consists of two parallel, 18-span bridges built in 1981 (northbound eastern bridge) and 1983 (southbound, western bridge) (Figure 21). Most of the 18 spans are 34 m long and 25 m wide (Wallace et al., 2001), with the exception of 40-m-long spans between the northern abutment and the first pair of piers. The bridge decks are supported by concrete piers on caisson foundations, which range in depth from 13 m to 16 m. The caissons on the hanging wall extending 5 to 10 m into shale bedrock of the Chinshui Formation, those on the footwall extend 16 m into coarse gravel alluvium (Figure 22). The piers for the western spans are circular in plan view (Figure 23), whereas the supports for the

eastern spans consist of wider pier walls. The one exception is Pier 3E on the eastern bridge, which consists of two smaller piers connected by a pier wall.

3.4.1 Description of Surface Rupture

As shown on Figure 21, the 1999 surface rupture crosses the Highway 3 Bridge near the northern margin of the active Wu Hsi floodplain. Across the southern part of the floodplain, the surface rupture consists of a single, 2-m-high fault scarp that is well expressed in the recent gravel alluvium (Kelson et al., 2001a). The scarp is nearly parallel to, and west of, the highway where it crosses the floodplain until encountering the bridge about 100 m south of the northern abutment (Figure 21). The fault intersects the third set of piers (Piers 3W and 3E; Figure WHB-1), where it splays into a complex series of smaller scarps that bend around individual piers. On the eastern side of the bridge, the individual fault strands re-join into a single strand that continues northward away from the river valley (Figure 21).

The characteristics of the surface fault rupture are substantially different in the vicinity of the bridge than elsewhere in the Wu Hsi valley. Southwest of the Wu Hsi and the Highway 3 bridge, the 1999 surface rupture consists of a single, well-defined scarp (Kelson et al., 2001a; Figure 21). Based on our detailed topographic profiling, the single scarp has a net vertical tectonic displacement (NVTD) of about 2 m south of the bridge (Profile DD', Figure 24d). Similarly, the topographic profile located across the fault zone north of the bridge indicates a NVTD of about 1.6 m and a simple, single fault scarp (Profile AA', Figures 24a and 25). Assuming a 30˚ fault dip, these profiles suggest about 2.8 to 3.2 m of horizontal shortening at this site during the 1999 rupture. Based on the morphology of the fault scarp and our observations of "bulldozed" plant material along the fault tip in the weeks following the earthquake, we interpret that the shortening occurred as hanging-wall run-out on the pre-rupture ground surface.

As the surface rupture approaches the piers from the south, it splits into several scarps that bend around individual piers (Figure 23). In particular, the eastern fault strand extends northward directly into Pier 3E (Figure26), wraps around the pier, and then continues northward. The western strand splits into several smaller scarps near Pier 3W, with the westernmost fault scarp bending several meters westward away from the pier footing (Figure 26). Topographic profile CC' crosses the fault zone south of Piers 3W and 3E, and shows the relative heights and displacements along the two major strands of the fault (Figure 24c). The net vertical tectonic displacement (NVTD) across the zone at this location is about 2.4 m, and the western scarp is slightly larger than the eastern scarp. Farther north along strike, the NVTD along topographic profile BB' is similar (about 2.4 m, Figure 24b), which is larger than the NVTD across the fault to the south of the bridge. Along both of the profiles beneath the bridge, we interpret that the western fault strand dips shallowly eastward and merges with the eastern fault strand in the shallow subsurface. Other possible interpretations of the subsurface geometry of the fault include the presence of two parallel, east-dipping fault strands, or a shallow western strand and a steep eastern strand that merges with the western strand at depth. Thus, it appears that individual surface-rupture scarps splayed around the bridge piers located within the fault zone.

Subsurface data along the bridge foundation provides additional information about the location of the Chelungpu fault across the Wu Hsi valley. As shown on Figure 22, the caisson foundations extend several meters into shale bedrock of the Chinshui Formation on the eastern

side of the fault. The coarse Holocene gravel alluvium east of the fault is approximately 3 to 7 m thick. In contrast, the caissons northwest of the fault extend at least 16 m into young alluvium and did not encounter bedrock (Figure 22). These data suggest that the location of the 1999 surface rupture coincides with the pre-1999 fault trace at this site, and that the Chelungpu fault has experienced recurrent Holocene surface rupture.

3.4.2 Bridge Damage

As noted above, individual surface-rupture scarps splayed around the bridge piers located within the fault zone. In particular, the eastern fault scarp extends directly into Pier 3E (Figure 26b), wraps around the pier, and then continues to the northeast (Figure 23). This pier, for an unknown reason, is different than the others supporting the eastern bridge spans, and consists of two smaller piers connected by a concrete pier wall. Where the fault tip meets the pier wall, the concrete contains a distinct upward-widening fracture that dips moderately (63˚) southeast (Figure 23 and 26b). This fracture likely formed as a result of west-vergent thrusting of the pier wall against the western pier, and consequent tilting of the western pier. As a result, the eastern bridge spans were thrust to the northwest and, as noted by Wallace et al. (2001), impacted the bridge decks of the western (southbound) bridge. In addition, the northwestward thrusting of the piers supporting the eastern bridge forced the bridge deck between piers 3E and 2E into the next adjacent deck to the north, which was pushed off it is support and collapsed (Figure 25; Kelson et al., 2001a; Wallace et al., 2001). The northernmost bridge deck on the eastern bridge also collapsed (Figure 25) as a result of being pushed northward off Pier 1E. The footwall deformation of the eastern structure also included shear failure of Pier 2E, which probably was a result of the large displacements transmitted through the bridge deck from Pier 3E. Wallace et al. (2001) note that the spans on both bridges showed large displacements and extensive damage at the expansion joints.

In contrast, the spans of the western (southbound) bridge remained supported, although the four northern piers supporting the western bridge experienced severe damage (Wallace et al., 2001). Piers 1W and 2W failed in shear involving nearly complete fracture of the pier (Figure 20b). Pier 3W, which coincides with one of the fault scarps, had cracking from torsion failure, and Pier 4W had a large flexural crack (Wallace et al., 2001). This distribution of damage is explained through analysis of the pattern of surface rupture. The western fault scarp extends northward directly into Pier 3W, where it then splays into a smaller scarp west of the pier, a scarp through the pier, and a scarp between Piers 3W and 3E (Figure 23). Because Pier 3W was located directly on the primary western fault strand, it failed in torsion related to northwest-vergent displacement of the thrust fault tip and, possibly, impact from the northwestward moving hanging-wall material. Because Pier 3W was structurally connected to Piers 2W and 1W via the western bridge decks, the northwestward displacement of Pier 3W imposed northward loads on, and caused shear failures of, Piers 2W and 1W. It appears that the structural connection of the bridge decks allowed the deformation along the fault rupture to be transmitted to the structures on the footwall. On the hanging wall, the large flexural crack in Pier 4W (noted by Wallace et al., 2001) likely was a result of extension, as was commonly observed on the hanging wall of the 1999 rupture (Kelson et al., 2001a, 2001b). This may be a result, in part, of a strong structural connection between adjacent bridge piers via the bridge decks, with Pier 4W being pulled northward by the movement of Pier 3W.

3.4.3 Interpretation of Patterns of Ground Deformation and Bridge Damage

Along the northbound (eastern) bridge, contraction generated by the fault displacement appears to have pushed the concrete spans northward off the piers, causing subsequent collapse (Figure 25). The southbound (western) spans did not collapse, although the spans and piers were severely damaged. In particular, the two piers on the footwall block closest to (but northwest of) the surface rupture (Piers 1W and 2W, Figure 23) experienced substantial shear failure (Wallace et al., 2001), although the closest pier on the hanging-wall block (Pier 4W) showed evidence of flexural cracking related to extension rather than shear failure. As with the eastern bridge spans, the damage to the eastern piers on the scarp and footwall probably are a result of west-directed contraction. As noted by Kelson et al. (2001), the weaker western piers may have helped prevent total collapse because they underwent severe plastic strain to accommodate fault displacement and allowed the spans to remain attached to the top of the piers. In contrast, the stronger eastern piers forced the displacement to occur at the interface between the pier and the bridge deck, resulting in unseating of the spans (Kelson et al., 2001).

Torsion failure of Pier 3W likely was related to uplift along the western strand of the fault zone, and northwestward thrusting. This, in turn, translated the northernmost two western bridge spans west and north toward the bridge abutment, and imposed large demands on Piers 1W and 2W, possibly contributing to the shear failures observed on these piers (Wallace et al., 2001; Kelson et al., 2001a). The flexural cracking of Pier 4W likely is related to hanging-wall extension as was commonly observed elsewhere along the fault rupture (Kelson et al., 2001a, 2001b). In addition, Wallace et al. (2001) attribute some of the structural damage of the western structure to westward translation of the eastern bridge deck into the western bridge deck.

4.0 CONCLUSIONS

The primary goal of this investigation is to evaluate the effects of ground deformation from the 1999 Chi-Chi earthquake on several buildings and other structures along the fault rupture. Because the earthquake produced surface rupture through densely populated areas, it provides an unprecedented opportunity to advance the understanding of the effects of surface fault rupture on engineered systems. All four of the sites studied in this investigation include structures that are either traversed by the surface rupture or are directly adjacent to the fault scarp. Two of the sites include buildings affected by the surface rupture, and two sites include either piers or a circular tower foundation.

At the Kuangfu Middle School site, a single well-defined fault scarp splays into three strands at the southeastern corner of the campus, where it first encounters a two-story classroom building. Overall, the net vertical displacement across the entire fault zone at this site is consistent from north to south, ranging from about 2.4 to 2.6 m. From north to south across campus, displacement along the fault is transferred from the eastern and central strands to the western strand. This transfer occurs where the fault traverses numerous buildings arranged with various orientations throughout the campus. In addition, we interpret from shallow borehole data that the location of the 1999 surface rupture does not coincide with the pre-1999 fault trace. These relationships suggest that the pattern of surface rupture in 1999 was affected by the location of classroom buildings on the campus. We speculate that this may be related, in part, to the ability of the classroom buildings to influence near-surface deformation of the relatively ductile, unconsolidated alluvial material in the shallow part of the hanging wall. In short, the location and orientation of the classroom buildings at Kuangfu Middle School probably influenced the pattern of ground rupture produced by the 1999 earthquake.

At the Experimental Vineyard site, the surface rupture traverses the vineyard but wraps around the southern end of a large factory building. We interpret that the massive concrete foundation of the factory building impeded the northwestward transport of the hanging wall and affected the location and height of the local surface scarp, resulting in localized folding on the hanging wall. The building experienced little or no structural damage even though the hanging wall material bulldozed into its southeastern corner. Based on our detailed mapping and subsurface borehole data, we interpret that the moderately strong factory building was able to withstand the load imposed by the thrusted hanging-wall material because of: (1) a footwall location, (2) a moderately competent building foundation, (3) an orientation of the building's long-axis roughly parallel to the thrust vergence direction, and (4) presence of unconsolidated, granular material in the uplifted and bulldozed hanging wall. Because the building affected the pattern of hanging-wall deformation, it may have significantly contributed to the severity of damage to nearby single-story residential buildings on the hanging wall.

At the Tsaotun Water Tower site, the fault rupture is expressed as a single, 1.5-m-high west-facing fault scarp that projects directly into the base of the 27-m-high water tower, wraps around the eastern side of the tower, and then continues to the northwest. Because the tower shows no evidence of structural damage or tilting, it appears that the surface rupture had no significant impact on the tower's structural integrity. Instead, we speculate that the splitting of the fault into

two strands north of the tower is related in some way to the northward direction of rupture propagation and the presence of the stable water tower, perhaps as a refraction of the rupture as it encountered the tower in the shallow subsurface. Thus, it appears that the presence of the water tower adjacent to the pre-1999 fault trace affected the distribution of deformation at the site, with the bulldozed soil on the hanging wall apparently squeezing around the sides of the tower during the earthquake rupture.

At the Wu Hsi Bridge site, the 1999 fault rupture south of the bridge consists of a single, 2-m-high fault scarp in floodplain alluvium. Near the northern abutment, the fault intersects the bridge piers and splays into a complex series of smaller scarps that bend around individual piers. On the eastern side of the bridge, the individual fault strands re-join into a single strand that continues northward. Our field observations suggest that the shortening occurred as hanging-wall run-out on the pre-rupture ground surface. The damage to the bridge piers and spans is directly related to west-vergent displacement and uplift along the fault, with shear failures in bridge piers coincident with west-directed contraction, and tension fractures in piers coincident with hanging-wall extension. Therefore, although the bridge piers are associated with caisson foundations that are more than 13 m deep, damage to the bridge as a result of the surface rupture was severe.

As a whole, the relationships between surface rupture and built structures at these four sites provide important information on the response of buildings and other structures to surface rupture. Buildings at the Kuangfu Middle School appear to have influenced the pattern of surface deformation and the number of individual fault scarps, although many of the buildings experienced severe damage. The Suncue Factory building at the Experimental Vineyard site also strongly influenced the pattern of fault rupture and the style of deformation on the hanging wall, thus also influencing damage to nearby buildings. In contrast, however, the Suncue Factory building experienced little or no damage. We speculate that this is related to the location of the buildings relative to the location of the pre-1999 fault trace, with severe damage occurring where buildings were located across the up-dip projection of the fault to the surface or on the hanging wall, as at Kuangfu Middle School. Where buildings are located completely on the footwall (west of the up-dip projection of the fault to the surface) damage was considerably less, as with the Suncue Factory. Similarly, severe damage occurred at the Wu Hsi Bridge where it traversed the Chelungpu fault trace, and experienced shortening as a result of spanning the primary width of deformation. The Tsaotun Water Tower was unaffected by the surface rupture, primarily because it is located on the footwall of the fault. In all four of the sites studied in this effort, the built structures influenced the pattern of fault rupture, and generally increased the width of the zone of substantial deformation.

5.0 REFERENCES

Azuma, T., and nine others, 1999, Geomorphological measurement on the fault scarp of 9/21 Taiwan earthquake [abs.]: Americal Geophysical Union 1999 Fall Meeting Program, Late Breaking Detailed Sessions, p. 13.

Bray, J. D., R. B. Seed and H. B. Seed, 1993a, Small-scale modelling of saturated cohesive soils: Geotechnical Testing Journal, American Society for Testing and Materials, v. 16, no. 1, p. 46-53.

Bray, J. D., A. Ashmawy, G. Mukhopadhyay and E. M. Gath, 1993b, Use of geosynthetics to mitigate earthquake fault rupture propagation through compacted fill: Proceedings of the Geosynthetics '93 Conference, v. 1, p. 379-392.

Bray, J. D., Seed, R.B., Cluff, L. S., and Seed, H. B., 1994a, Earthquake fault rupture propagation through soil: Journal of Geotechnical Engineering, ASCE, v. 120, no. 3, pp. 543-561.

Bray, J. D., R. B. Seed and H. B. Seed, 1994b, Analysis of earthquake fault rupture propagation through cohesive soil: Journal of Geotechnical Engineering, ASCE, vol. 120, no. 3, pp. 562-580.

Chen, W.-S., and Chen, Y.-G., 1999, The characteristics of surface ruptures in association with 1999 Chichi earthquake in Taiwan [abs.]: American Geophysical Union 1999 Fall Meeting Program, Late Breaking Detailed Sessions, p. 13.

Chen, Y.-G., Chen, W.-S., Lo, P.-W., Lee, C.-C., and Liu, T.-K., 1999, Fault movement caused geomorphic features: a case of Taiwan earthquake on Sep. 20, 1999 [abs.]: Americal Geophysical Union 1999 Fall Meeting Program, Late Breaking Detailed Sessions, p. 13.

Kelson, K.I., Lee, C.-T., Kang, K.-H., and Page, W.D., 2000a, Styles of surface deformation along the Chelungpu fault resulting from the 1999 Chi-Chi earthquake [abs.]: Symposium on Mitigation of the Risk of Surface Faulting, sponsored by the Taiwan National Science Council, National Central University, and Geophyscial Society of China; ChungLi, Taiwan, April 6-7, 2000.

Kelson, K.I., Kieffer, S., Sitar, N., Wright, R., Wells, D., and Perkins, W., 2000b, Fault-related deformation resulting from the Chi-Chi (Taiwan) earthquake: Preliminary conclusions of the NSF-PEER reconnaissance team [abs.], Seismological Society of America Annual Meeting, San Diego.

Kelson, K.I. (coordinator) and 13 other contributors, 2001a, Fault-related surface deformation: *in* Uzarski, J., and Arnold, C. (eds.), Chi-Chi, Taiwan, Earthquake of September 21, 1999 Reconnaissance Report: *Earthquake Spectra*, Earthquake Engineering Research Institute, Supplement A to v. 17, p. 19-36.

Kelson, K.I., Kang, K.-H., Page, W.D., Lee, C.-T., and Cluff, L.S., 2001b, Representative styles of deformation along the Chelungpu fault from the 1999 Chi-Chi (Taiwan) earthquake: Geomorphic characteristics and responses of man-made structures: Bulletin of the Seismological Society of America, v. 91, no. 5, p. 930-952.

Lade, P.V. and Cole, D. A., Jr., 1984, Influence zones in alluvium over dip-slip faults: Journal of Geotechnical Engineering, ASCE, Vol. 110, No. 5, p. 599-615.

Lazarte, C.A., J. D. Bray, A. M. Johnson and R. E. Lemmer, 1994, Surface breakage of the 1992 Landers earthquake and its effects on structures: Bulletin of the Seismological Society of America, Vol. 84, No. 3, p. 547-561.

Lazarte, C.A. and Bray, J.D., 1996, A study of strike-slip faulting using small-scale models: Geotechnical Testing Journal, American Society for Testing and Materials, v. 19, no. 2, pp. 118-129.

Lee, C.-T., Chang, C.-T., and Hsu, S.-K., 1999, Fault rupture associated with the September 21, 1999 Chichi earthquake, west central Taiwan [abs.]: American Geophysical Union 1999 Fall Meeting Program, Late Breaking Detailed Sessions, p. 14.

Ma K.-F., Lee, C.-T., Tsai, Y.-B., and Shin, T.-C., 1999, The Chi-Chi, Taiwan earthquake: Large surface displacements on an inland thrust fault: EOS, Transactions, American Geophysical Union, v. 80, no. 50, p. 605.

Murbach, D., Rockwell, T. K., and Bray, J. D., 1999, The relationship of foundation deformation to surface and near-surface faulting resulting from the 1992 landers earthquake: Earthquake Spectra, Earthquake Engineering Research Institute, v. 15, no. 1, pp. 121-144.

Sherard, J. L., Cluff, L. S., and Allen, C. R., 1974, Potentially active faults in dam foundations: Geotechnique, v. 24, p. 367-427.

Wallace, J.W. (coordinator), Eberhard, M.O., Hwang, S.-J., Moehle, J.P., Post, T., Roblee, C., Stewart, J.P., and Yashinsky, M., 2001, Highway bridges: *in* Uzarski, J., and Arnold, C. (eds.), Chi-Chi, Taiwan, Earthquake of September 21, 1999 Reconnaissance Report: *Earthquake Spectra*, Earthquake Engineering Research Institute, Supplement A to v. 17, p. 131-152.

Youd, T. L., 1989, Ground failure damage to buildings during earthquakes: *in* Foundation Engineering--Current Principles and Practices, American Society of Civil Engineers, New York, v. 1, pp. 758-770.

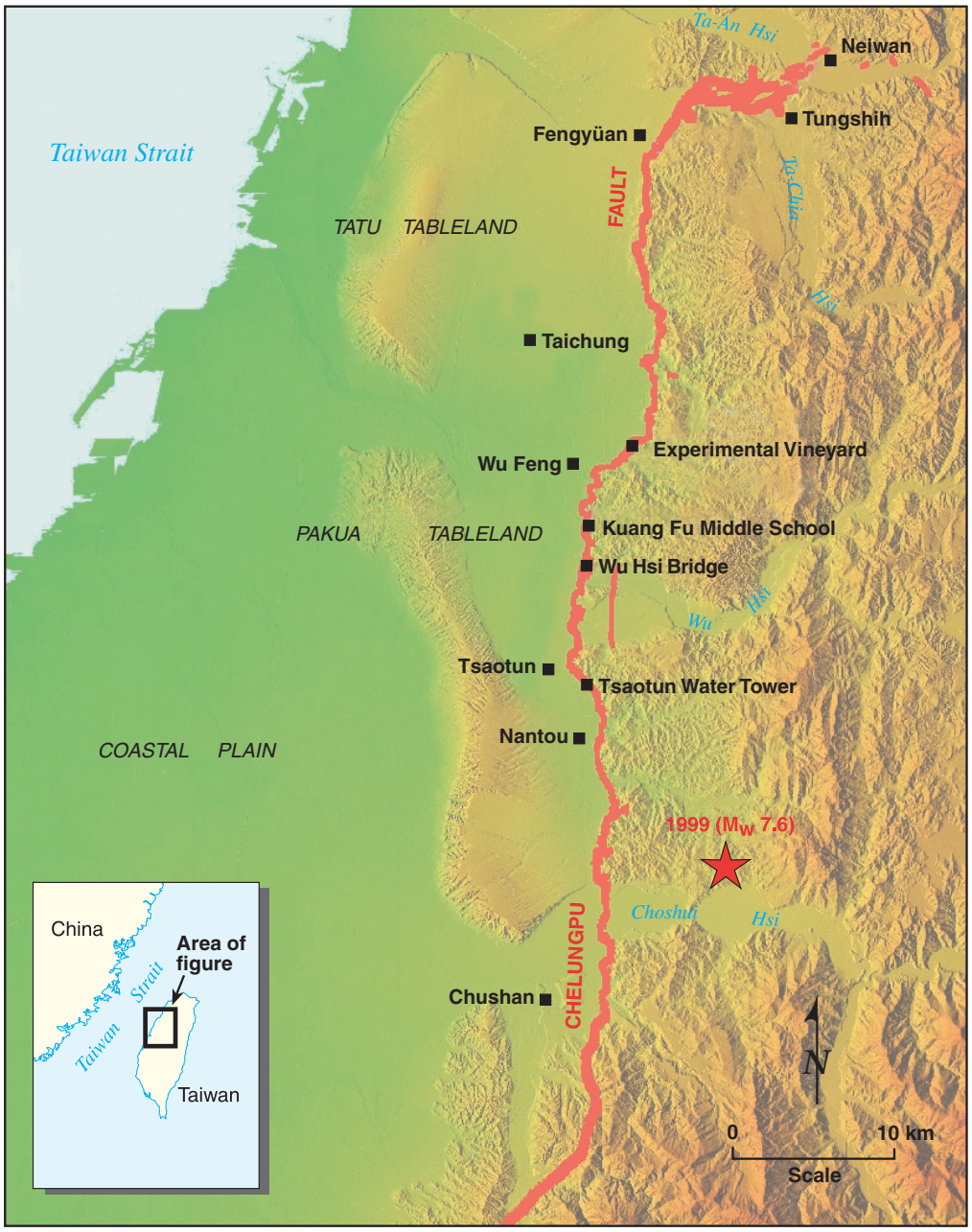

Figure 1. Digital elevation model of west-central Taiwan, showing the 1999 rupture trace of the Chelungpu fault, and sites investigated in detail in this study.

Figure 2a. Photograph of building on crest of Chelungpu fault scarp near Fengyüan, showing damage to thin-slab foundation. Vertical uplift at this site is 4m. Note multiple cracks in foundation.

Figure 2b. Photograph of Chelungpu fault near Fengyüan, showing structure tilted by thrust faulting and uplift of about 4m. Building at left is of similar construction, but was relatively undamaged because of location on footwall.

Figure 2c. Photograph of Chelungpu fault scarp near Fengyüan, showing uplift on fault of about 4m.

Figure 3. Photograph looking south along Chelungpu fault rupture in Wu Feng. The fault rupture passed beneath this apartment building, producing displacement of the building. [Photo taken; October 11, 1999].

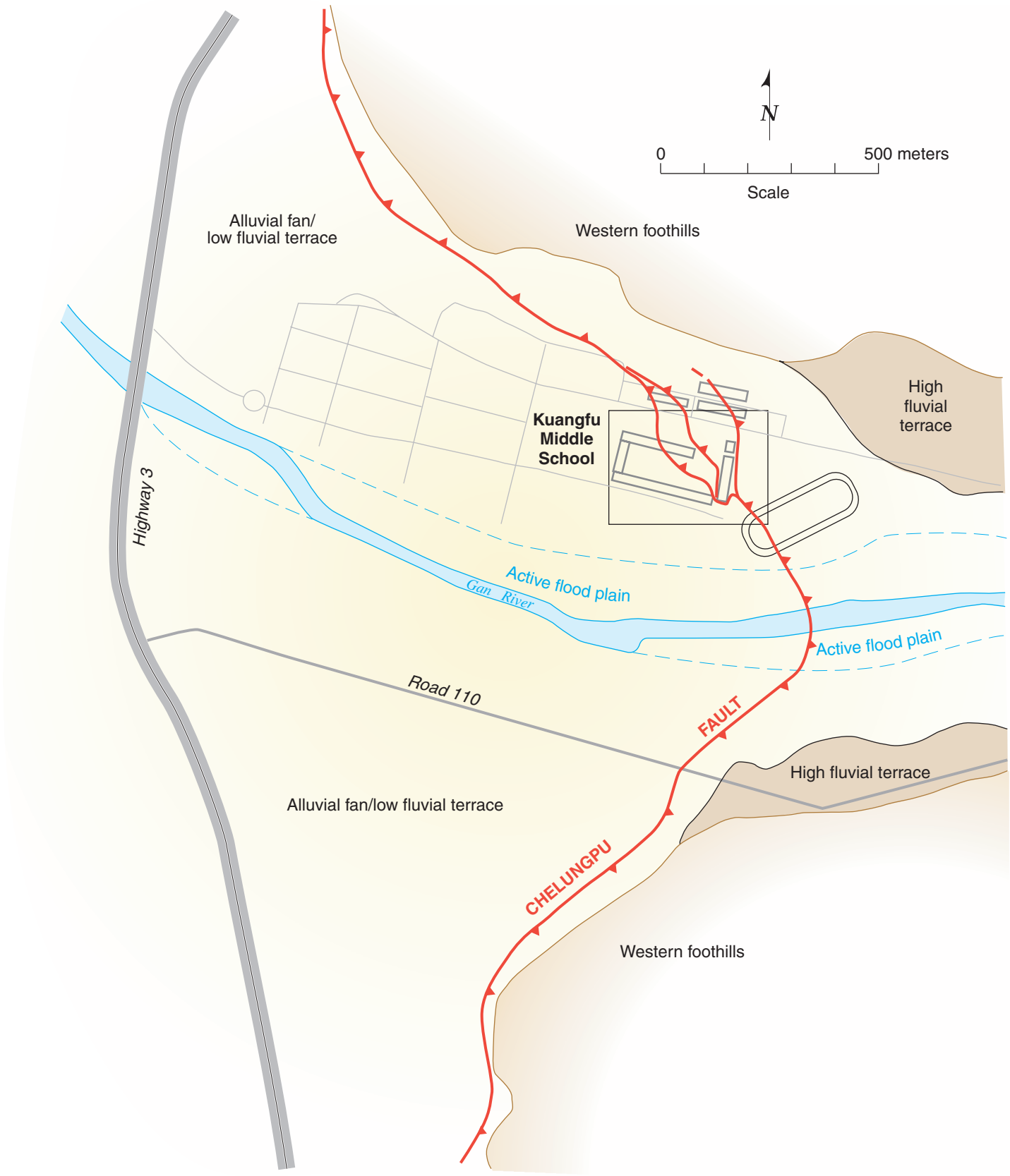

Figure 4. Generalized geologic map of the Chelungpu fault in the vicinity of Kuangfu Middle School, south of Wu Feng. The trace of the 1999 surface rupture modified from mapping by the Taiwan Central Geological Survey mapping.

Figure 5. Photograph of 3 meter high fault scarp crossing the Kuangfu Middle School track and field. Eastern Classroom building is behind trees in background, and has the tilted water tank on its roof (photo taken October 11, 1999).

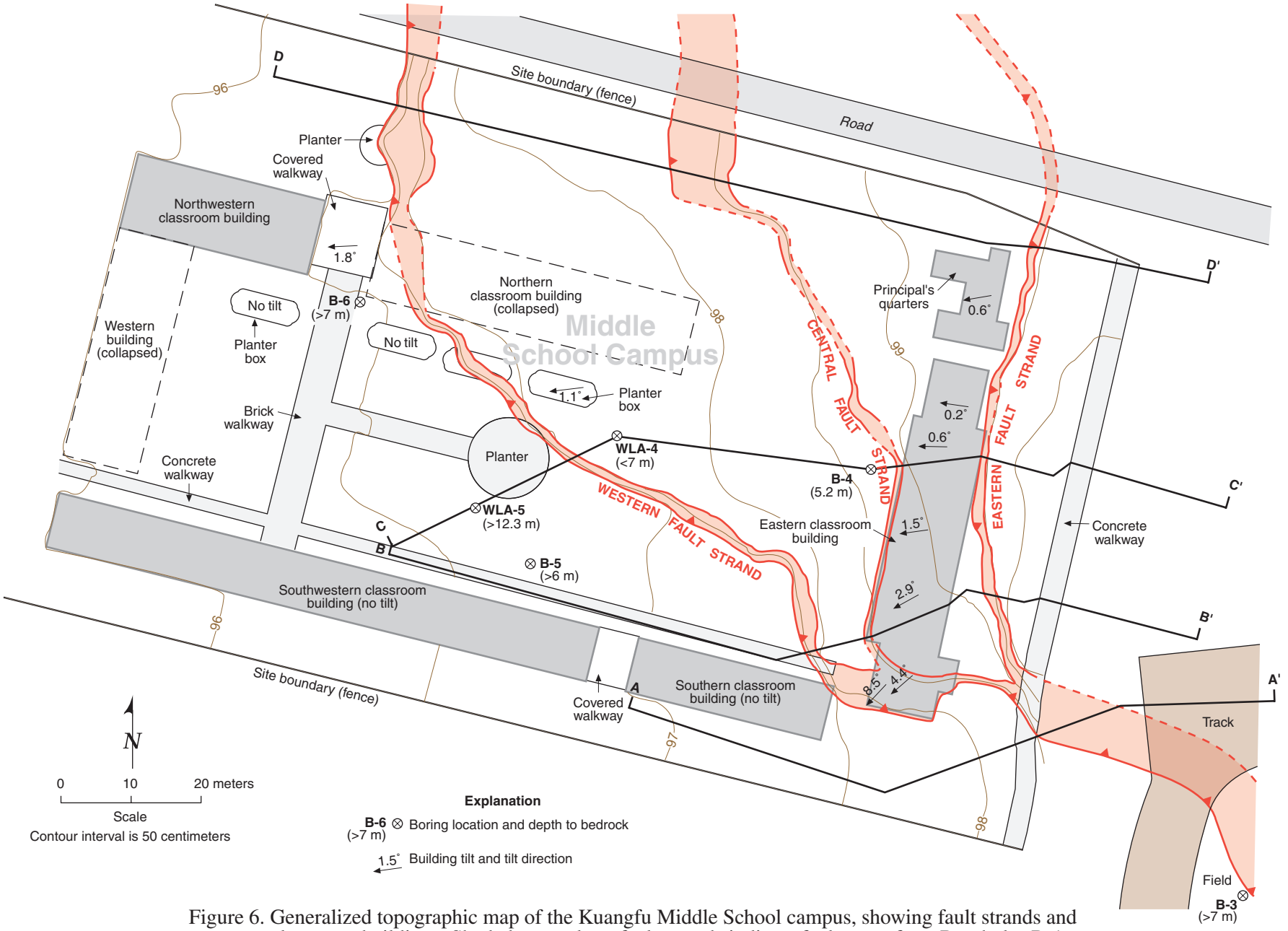

Figure 6. Generalized topographic map of the Kuangfu Middle School campus, showing fault strands and classroom buildings. Shaded areas along fault strands indicate fault scarp face. Boreholes B-1 and B-2 are located on playing field, southeast of B-3.

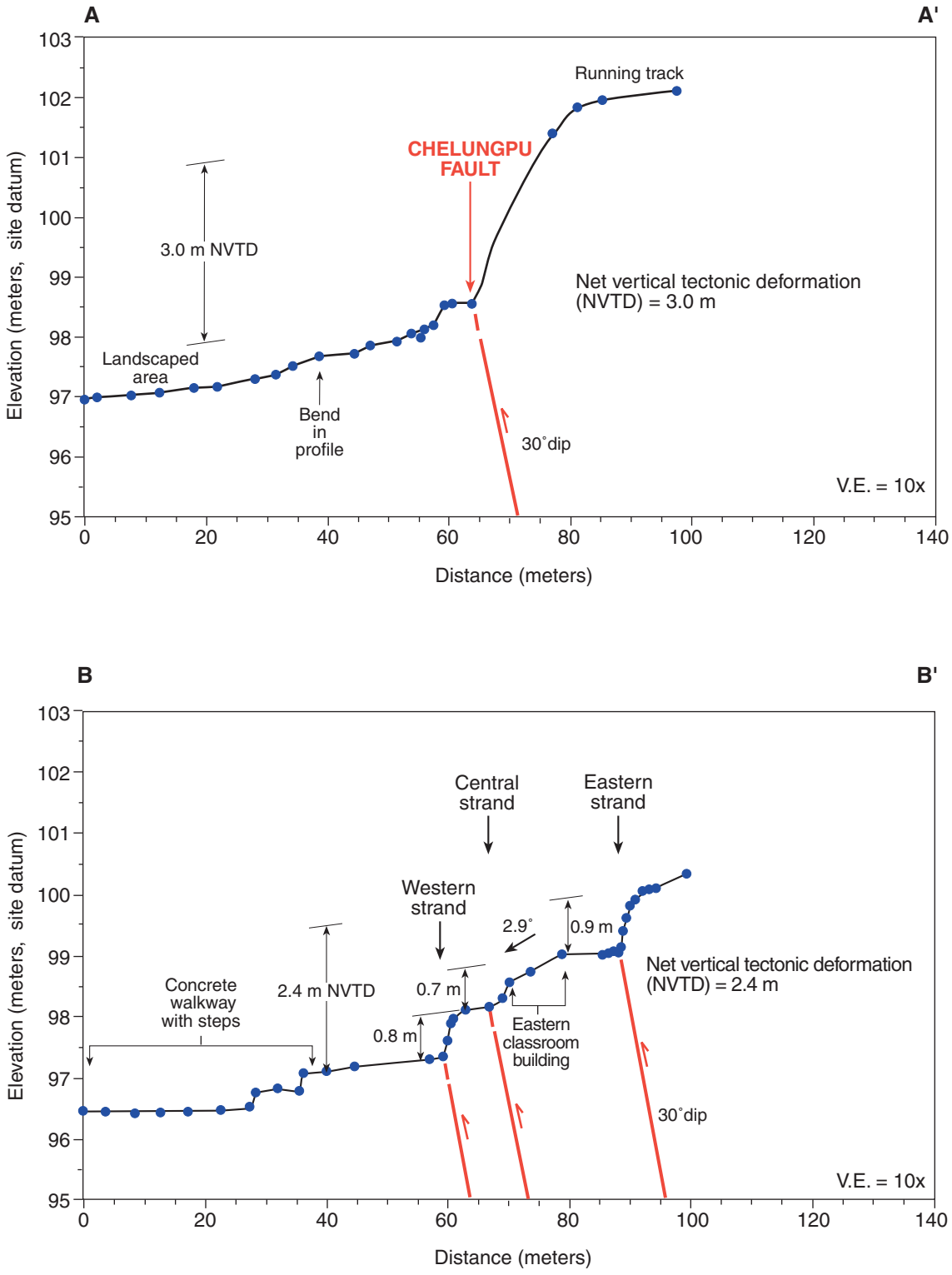

Figure 7. Topographic profiles AA' and BB', Kuangfu Middle School. Fault dip of 30˚E is assumed. See Figure 6 for profile locations.

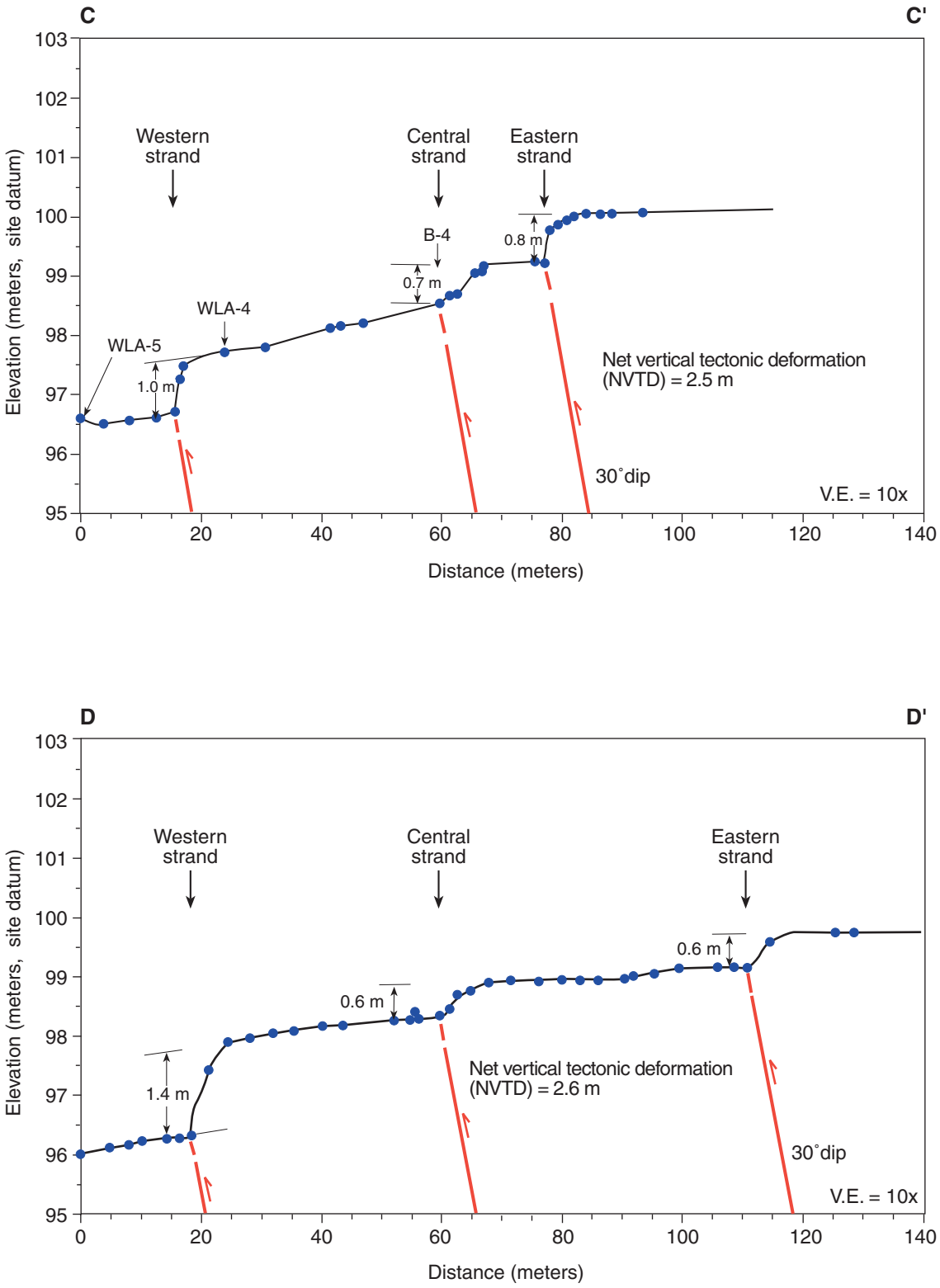

Figure 8. Topographic profiles CC' and DD', Kuangfu Middle School. Fault dip of 30˚E is assumed. See Figure 6 for profile locations.

Figure 9a. Photograph looking south along eastern fault strand on the eastern side of the Eastern Classroom building, Kuangfu Middle School (photo taken June 8, 2001).

Figure 9b. Photograph looking north along eastern fault strand, along eastern side of Eastern Classroom building (photo taken April 11, 2000).

Figure 10a. Photograph of western fault strand at Kuangfu Middle School where it goes between the Eastern Classroom building, on left, and the Southern Classroom Building, on right (photo taken September 7, 2001).

Figure 10b. Photograph of western fault strand where it encounters the Eastern Classroom building (photo taken April 11,2000).

Figure 11a. Photograph looking northeast toward the collapsed Northern Classroom building at Kuangfu Middle School, across the western fault strand (photo taken April 11, 2000).

Figure 11b. Photograph looking southeast toward the collapsed Northern Classroom building at Kuangfu Middle School, along the western fault strand (photo taken September 9, 2001).

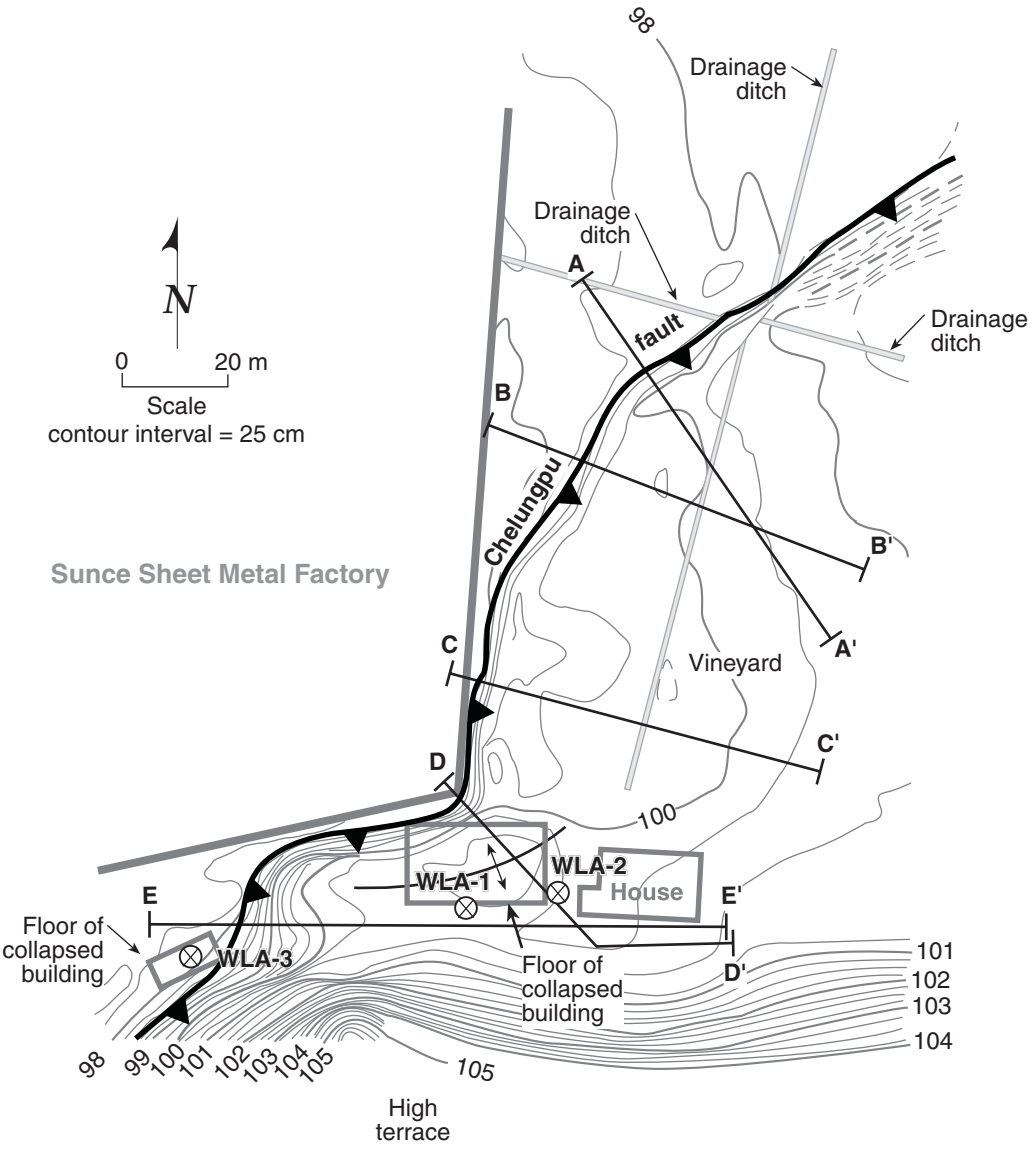

Figure 12. Topographic map of the Experimental Vineyard site, showing Chelungpu fault scarp, topographic profile locations, existing buildings, and boreholes (WLA-1, WLA-2, and WLA-3) completed in this study. Modified from Kelson et al. (2001b).

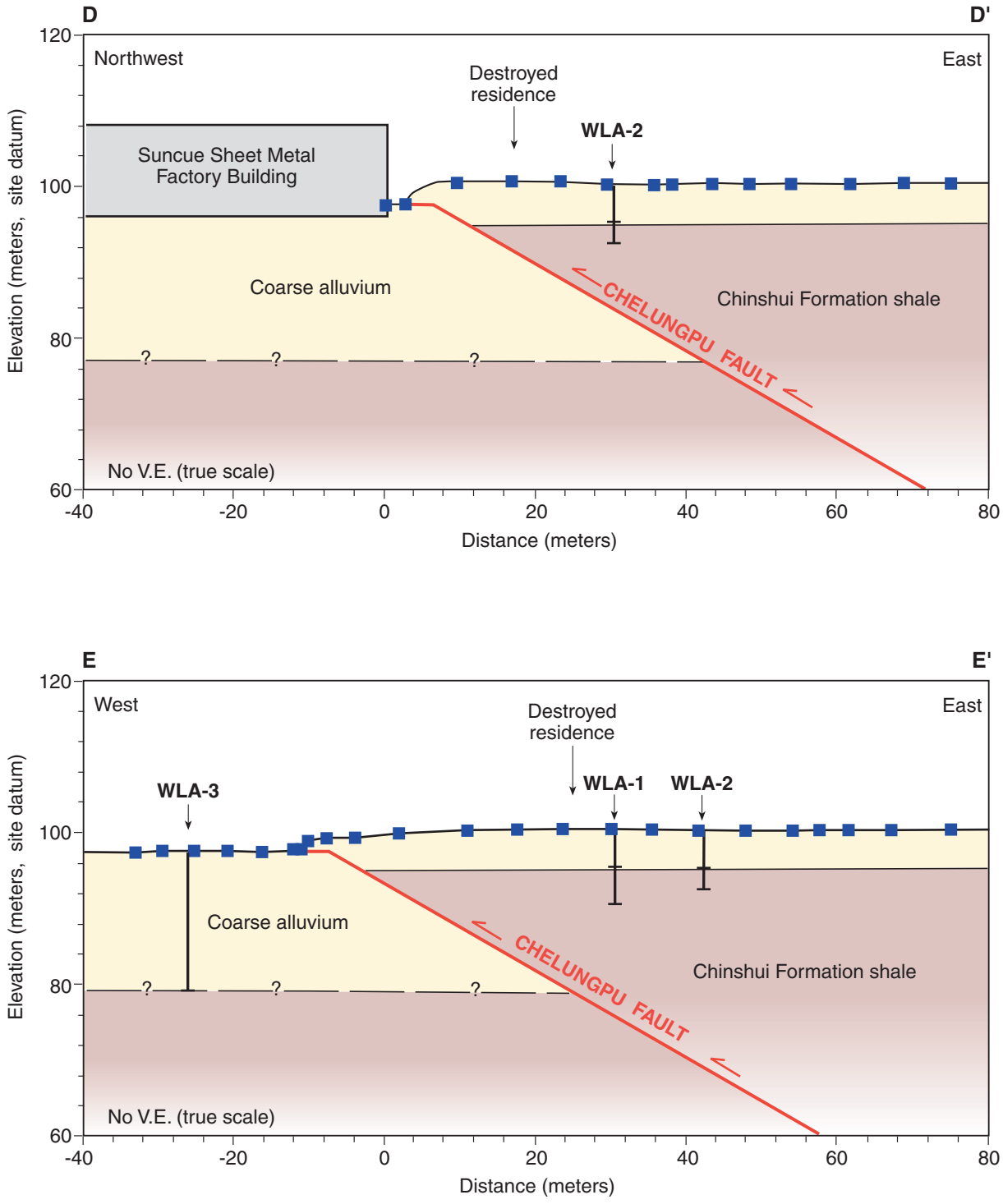

Figure 13. Topographic profiles DD' and EE' at the Experimental Vineyard site, showing shallow geologic conditions based on boreholes WLA-1 through WLA-3. See Figure 12 for locations.

Figure 14. Photograph of Tsaotun Water Tower looking east (photo taken June 9, 2001). Chelungpu fault is in shadows behind tower (not visible).

Figure 15. Generalized topographic map of the Tsaotun water tower site, showing fault strands, and location of water tower. Shaded areas along fault strands indicate fault scarp.

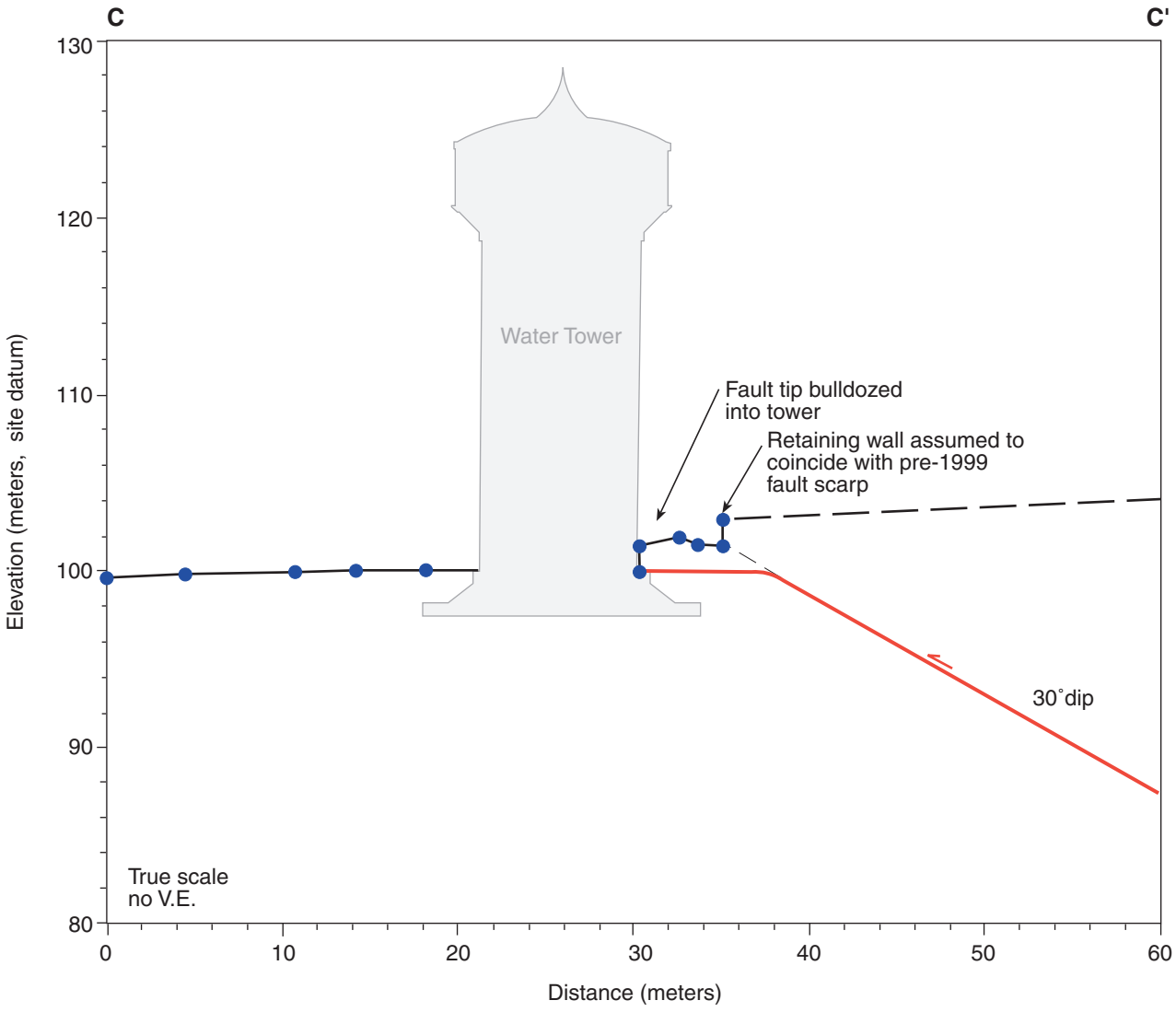

Figure 16. True-scale topographic profile CC' at the Tsaotun Water Tower site, showing tower structure and foundation based on as-built plans, and inferred location of the Chelungpu fault (assumed 30˚ dip). See Figure 15 for location of CC'.

Figure 17a. Photograph looking northeast toward the Tsaotun Water Tower and along the Chelungpu fault, showing tilted trees on scarp face south of tower (photo taken June 9, 2001).

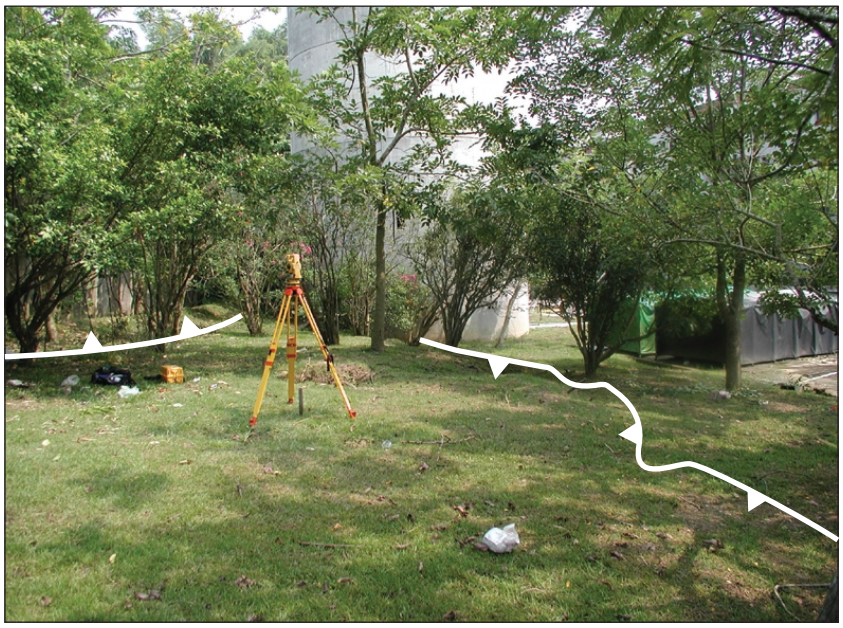

Figure 17b. Photograph looking south toward the Tsaotun Water Tower from hanging wall of the western fault strand. Eastern fault strand shown on left side of photograph (photo taken September 10, 2001).

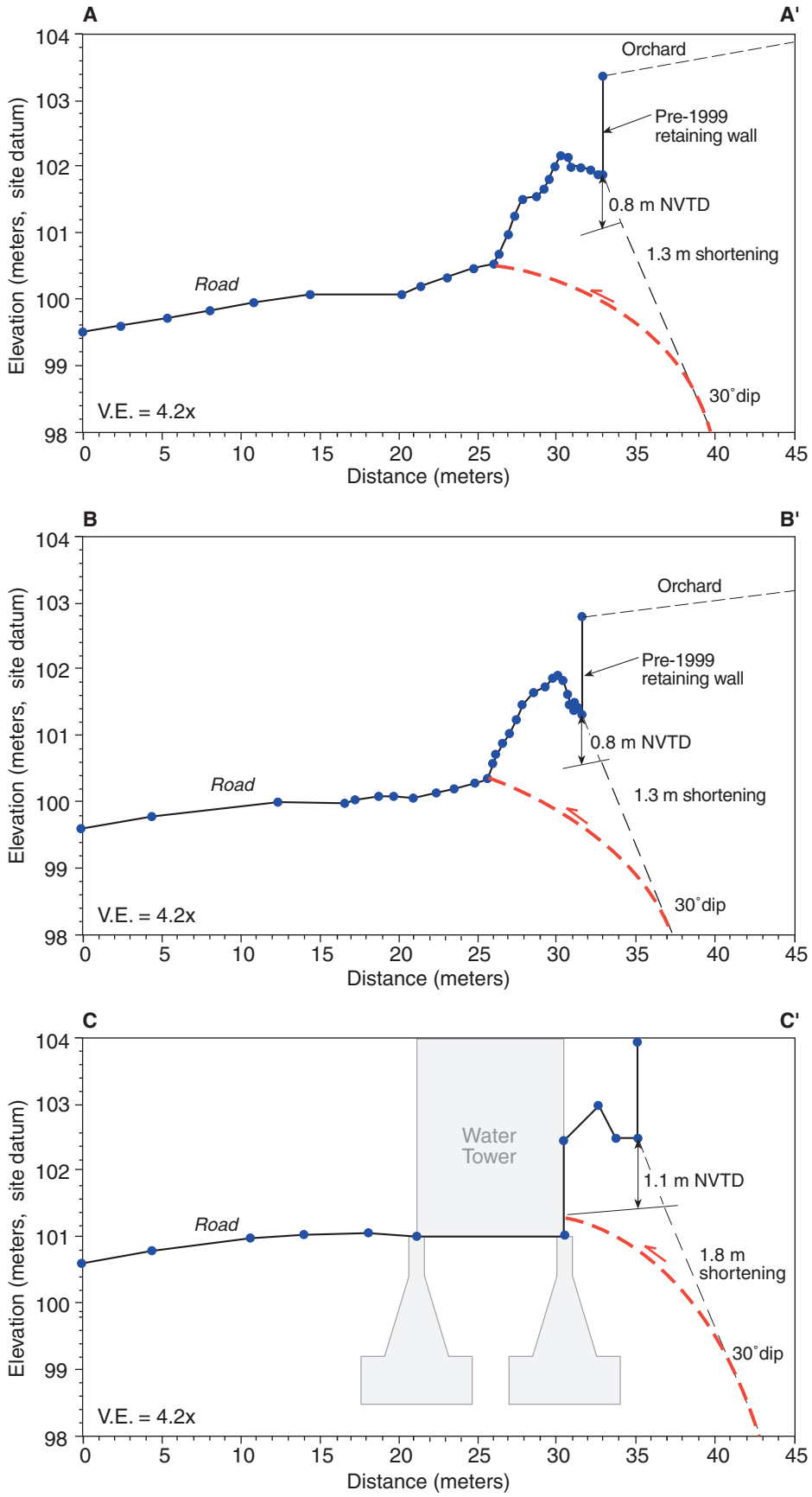

Figure 18. Topographic profiles AA' through CC', Tsaotun Water Tower site. Fault dip of 30˚ is assumed. See Figure 15 for profile locations.

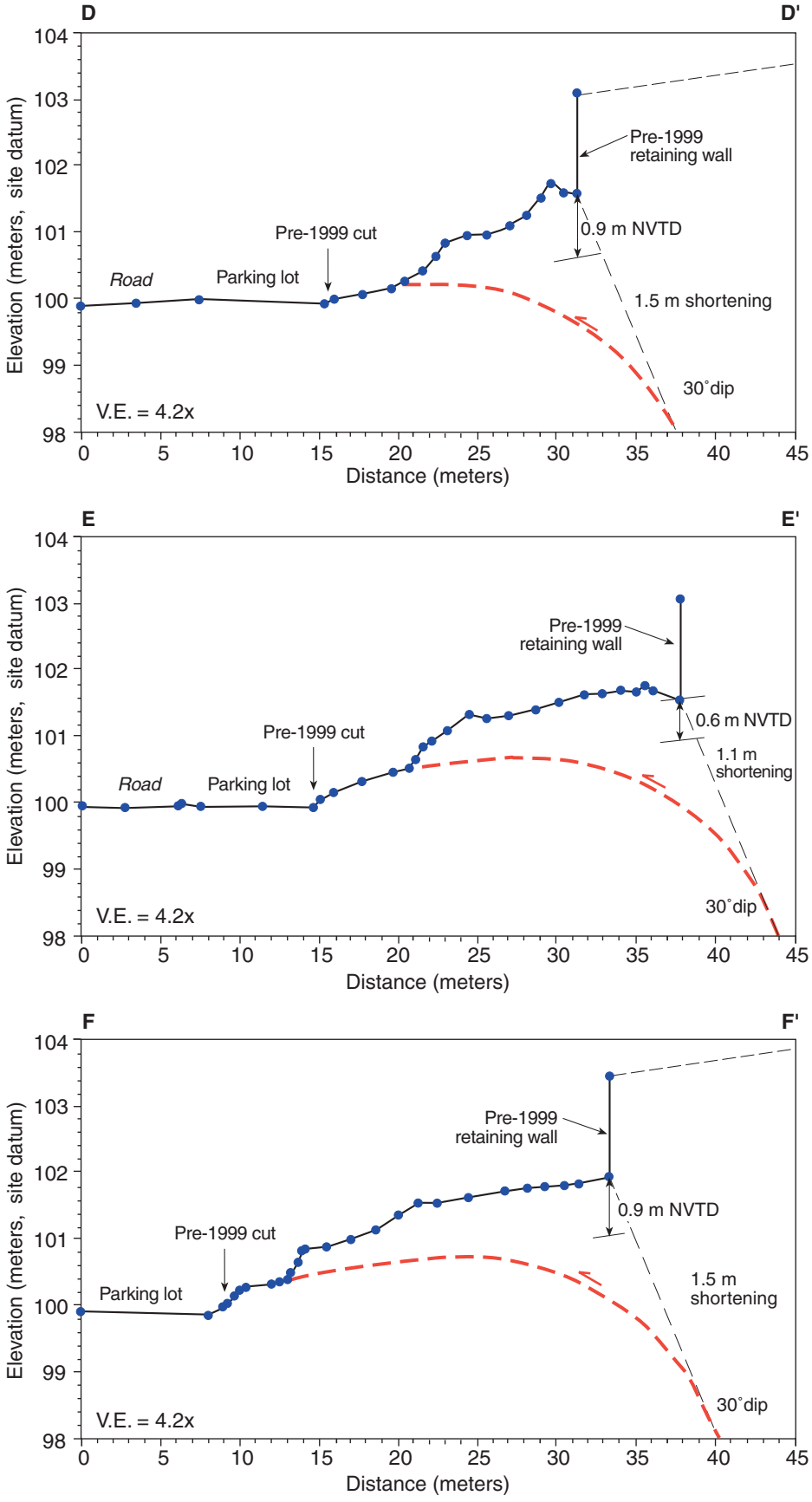

Figure 19. Topographic profiles DD' through FF'. Fault dip of 30˚ is assumed. See Figure 15 for profile locations.

Figure 20a. Photograph looking south along the Wu Hsi Bridge, showing shear fractures in Piers 1W and 2W and two collapsed spans of eastern bridge. Note uplifted bridge spans south of Piers 4W in background (photo taken October 12, 1999).

Figure 20b. Photograph looking southeast at the northern part of the Wu Hsi Bridge, showing shear fractures in Piers 1W and 2W. The Chelungpu fault strands run through piers 3W, and 3E, which are tilted toward the viewer (photo taken October 12, 1999).

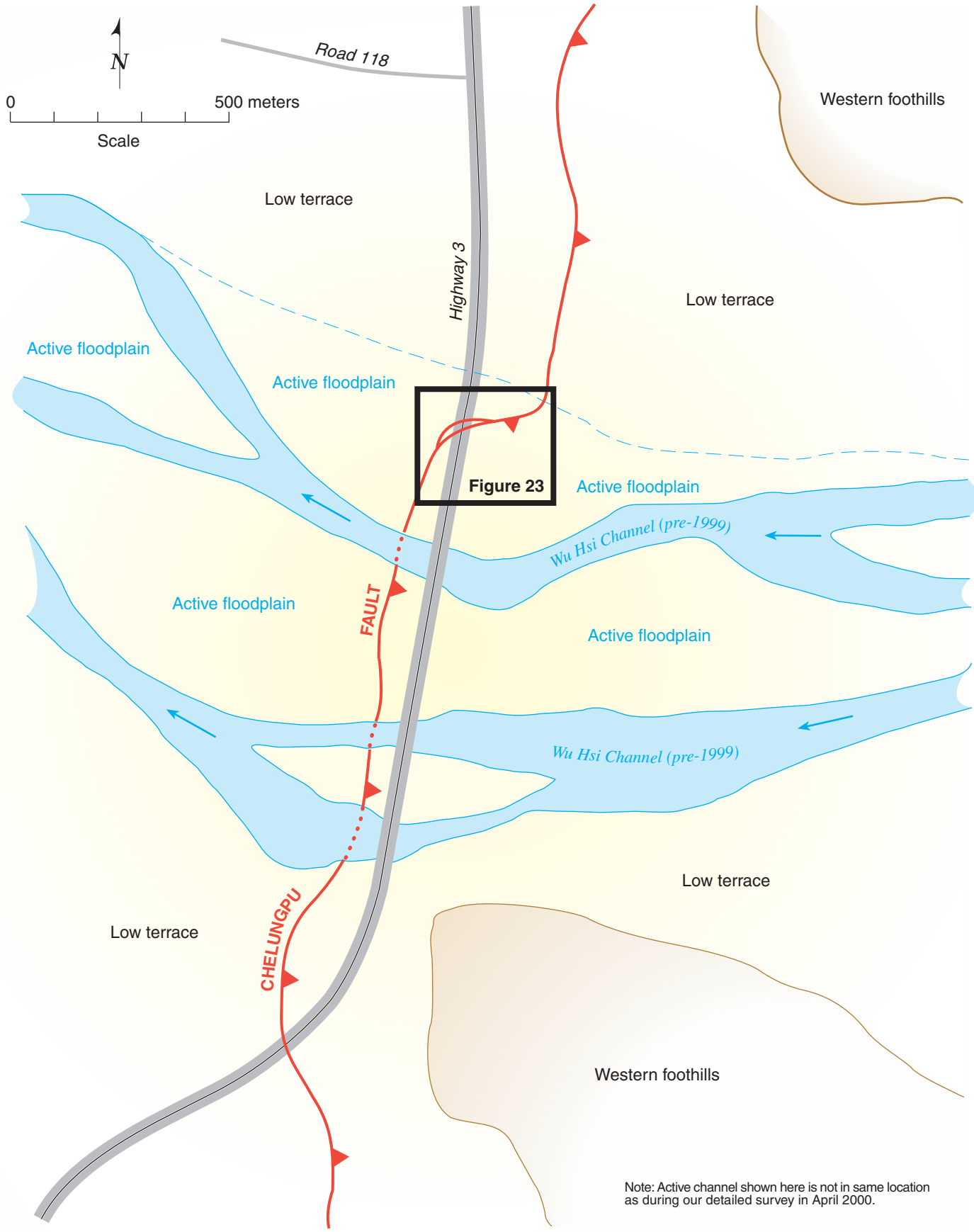

Figure 21. Generalized geologic map of the Chelungpu fault in the vicinity of the Wu Hsi Bridge. The trace of the 1999 surface rupture is modified from mapping by the Taiwan Central Geological Survey.

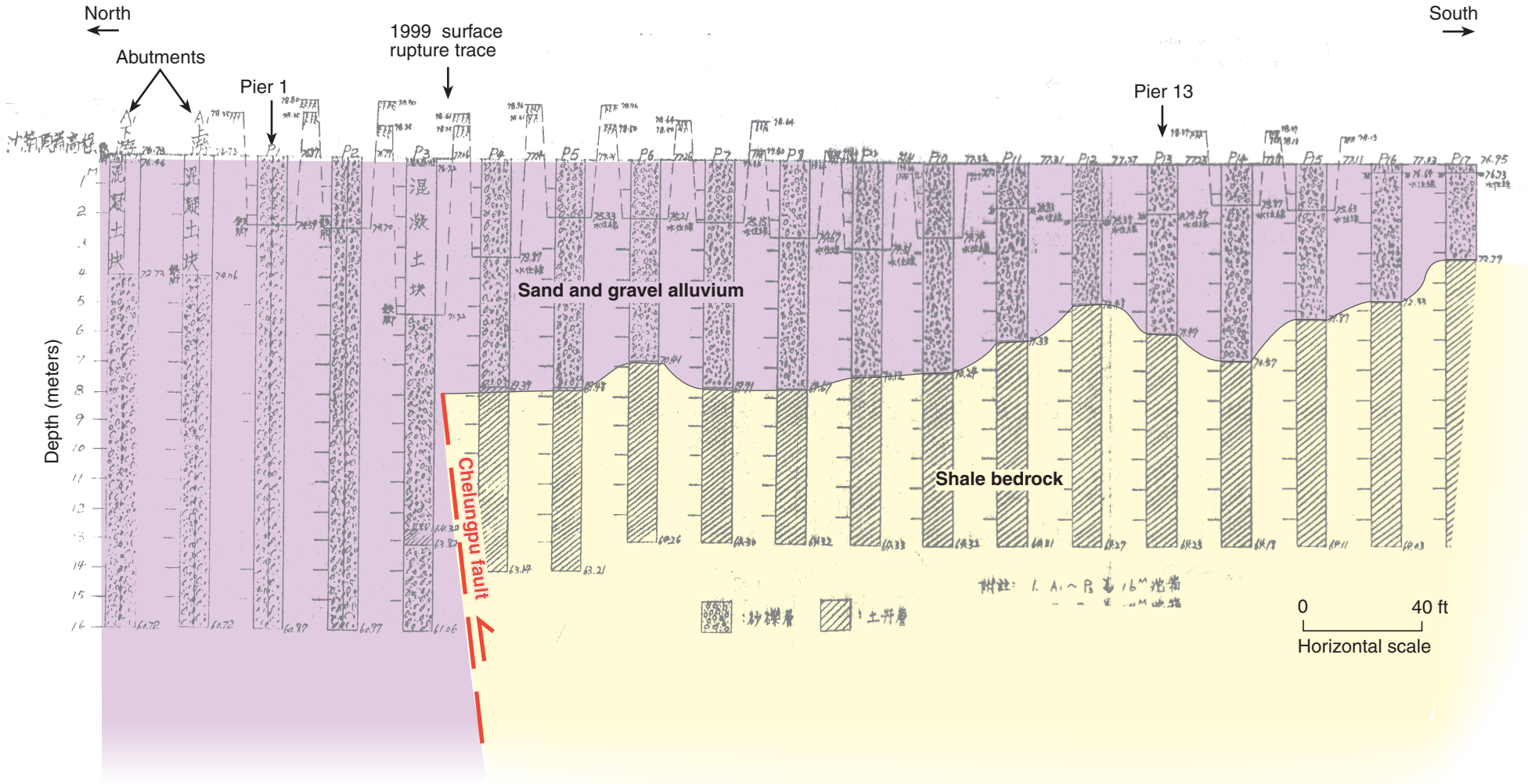

Figure 22. Geologic cross section at Wu Hsi Bridge prior to the 1999 Chi-Chi earthquake, based on logs of excavations for pier caissons.

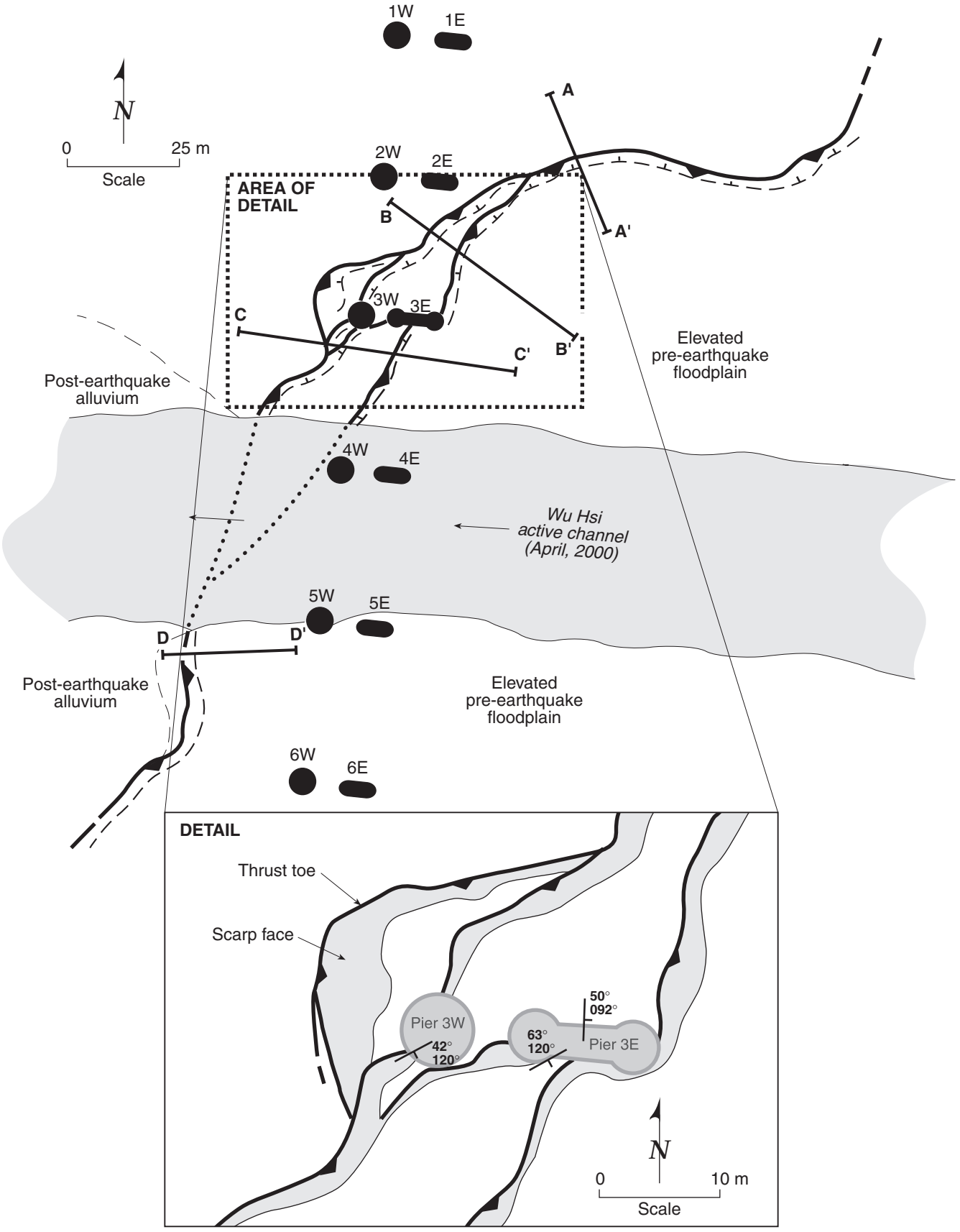

Figure 23. Detailed map of the 1999 Chelungpu fault rupture through the Wu Hsi Bridge, showing locations of bridge piers, fault strands, and topographic profiles. Inset map shows details of fault rupture near Piers 3w and 3E, and orientations of fractures developed in the piers.

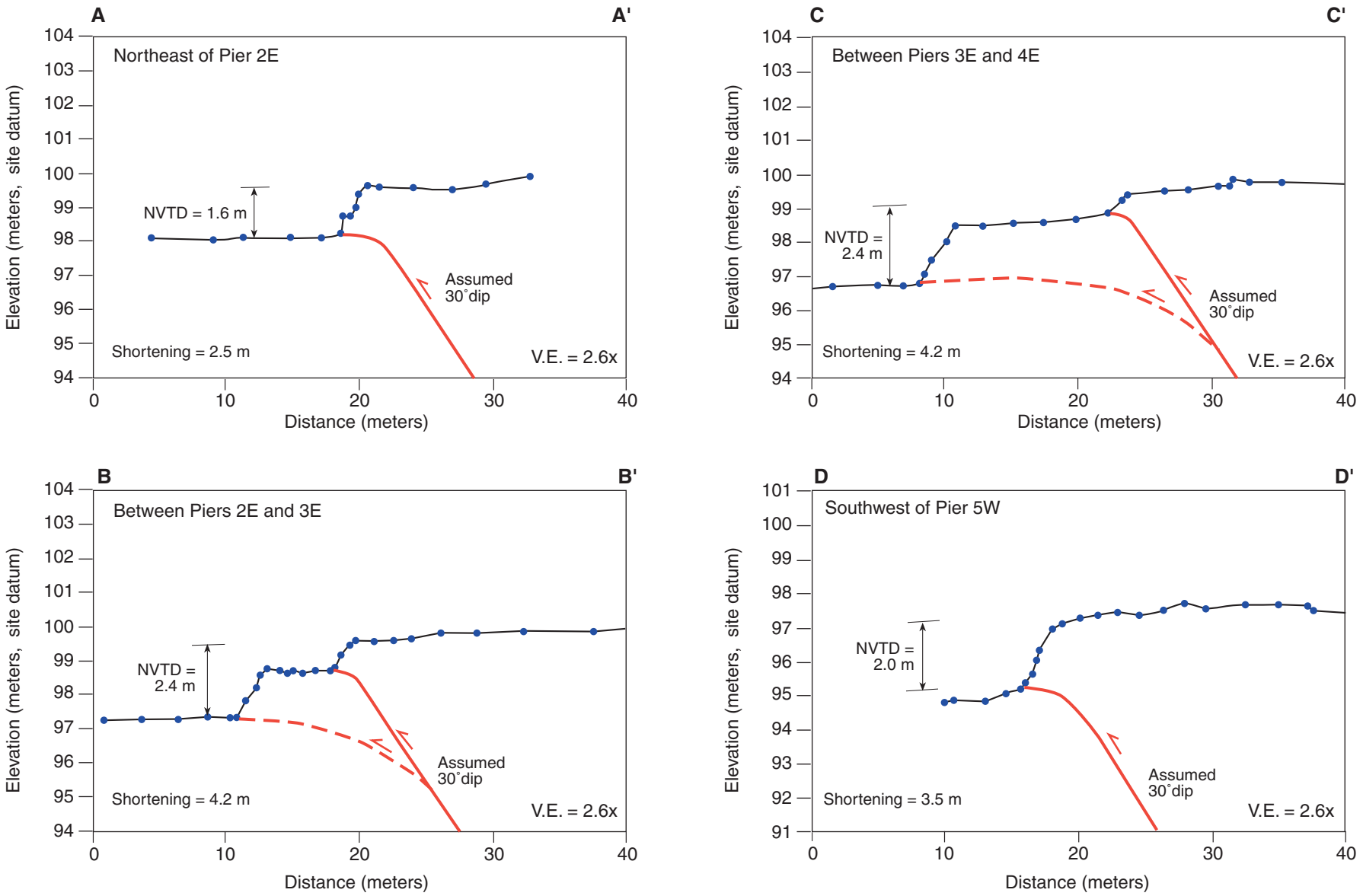

Figure 24. Topographic profiles across the Chelungpu fault at Wu Hsi Bridge. See Figure 23 for locations of profiles.

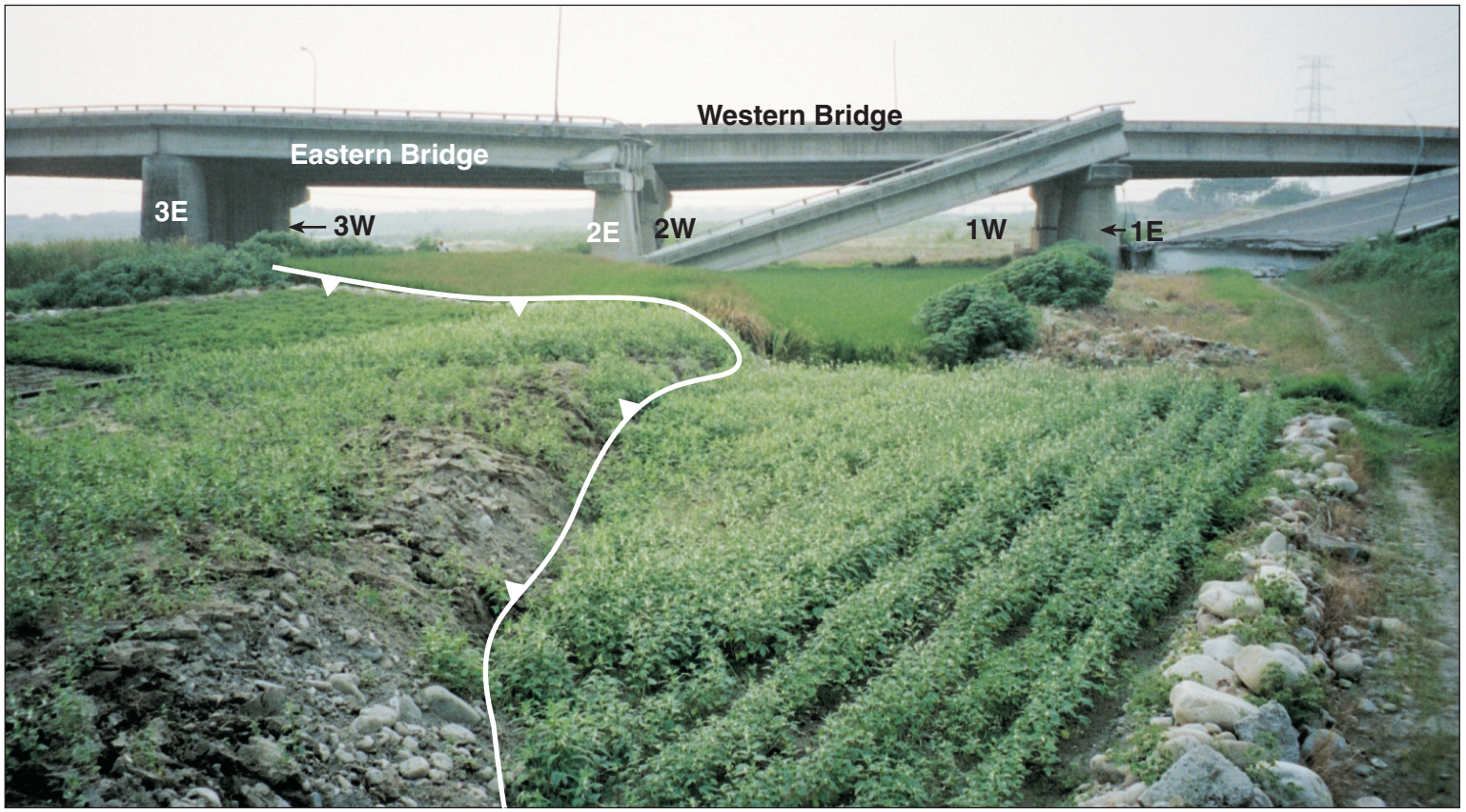

Figure 25. Photograph looking west of the northern part of the Wu Hsi Bridge, showing Chelungpu fault scarp in foreground and Highway 3 in background. The two collapsed northernmost spans of the northbound (eastern) bridge are on right side of photograph. (photo taken October 12, 1999).

A)

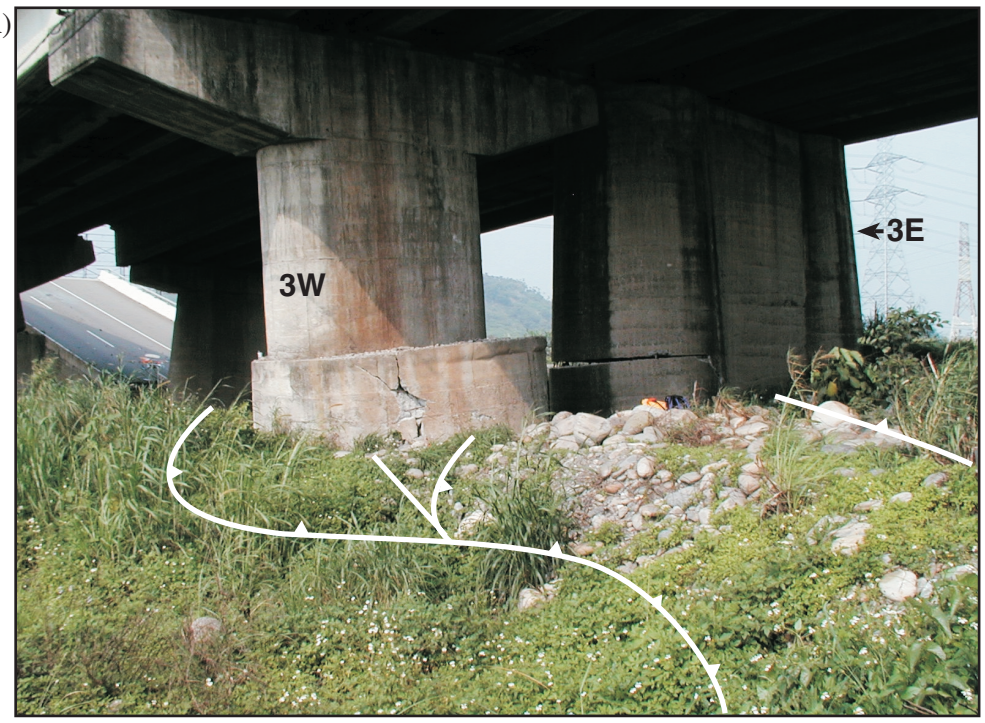

Figure 26a. Photograph looking northeast along western strand of Chelungpu fault at the Wu Hsi Bridge site, showing west-facing fault scarps and damage to Piers 3W and 3E. Collapsed bridge span and Pier 2E in left background (photo taken April 9, 2000).

B)

Figure 26b. Photograph looking north at Pier 3E along the eastern fault strand, showing east-dipping fracture in pier and west-facing fault scarp (photo taken April 15, 2000).